UCRL-53576
Distribution Category UC-70

Report on Static Hydrothermal Alteration Studies of Topopah Spring Tuff Wafers in J-13 Water at 150°C

K. G. Knauss

W. B. Beiriger

Manuscript date: August 31, 1984

LAWRENCE LIVERMORE NATIONAL LABORATORY
University of California • Livermore, California • 94550

Available from: National Technical Information Service • U.S. Department of Commerce
5285 Port Royal Road • Springfield, VA 22161 • $8.50 per copy • (Microfiche $4.50)

Contents

Report on Static Hydrothermal Alteration Studies of Topopah Spring Tuff Wafers in J-13 Water at 150°C

Abstract

This report presents the results of preliminary experimental work done to define the package environment in a potential nuclear waste repository in the Topopah Spring Member of the Paintbrush Tuff. The work is supported by the Nevada Nuclear Waste Storage Investigations (NNWSI) Project as a part of the Waste Package task to design a package suitable for waste storage within volcanic units at the Nevada Test Site.

Static hydrothermal alteration experiments were run for 4 months using polished wafers either fully submerged in an appropriate natural ground water or exposed to water-saturated air with enough excess water to allow refluxing. The aqueous results agreed favorably with similar experiments run using crushed tuff, and the use of solid polished wafers allowed us to directly evaluate the effects of reaction on the tuff. The results are preliminary in the sense that these experiments were run in Teflon-lined, static autoclaves, whereas subsequent experiments have been run in Dickson-type gold-cell rocking autoclaves. The results predict relatively minor changes in water chemistry, very minor alteration of the host rock, and the production of slight amounts of secondary minerals, when liquid water could return to the rock pores following the temperature maximum during the thermal period.

Introduction

The NNWSI Project has chosen the Topopah Spring tuff as the candidate horizon for a potential high-level nuclear waste repository to be located at Yucca Mountain, Nevada. The Waste Package task has been charged with designing an appropriate waste package and thus must understand the environment surrounding the package. The emplacement of the waste will alter the environment and this new hydrothermal environment must also be understood to predict waste form and package performance. To investigate the post-emplacement environment, we studied the changes in water chemistry and rock chemistry/mineralogy as a result of hydrothermal interaction. These studies also provide data needed to develop the geochemical modeling codes that will be used to make long-term predictions of conditions in the package environment.

The necessity for doing some of these hydrothermal experiments using outcrop samples of Topopah Spring tuff has been explained elsewhere (Knauss, 1984b). To accurately define the hydrothermal repository environment, analogous experiments are being run using drillcore samples taken from the stratigraphic depth of the potential repository horizon.

These static experiments using polished wafers were designed to complement analogous experiments (Oversby, 1984), which used crushed tuff. When this study is considered in conjunction with these other studies, we can determine:

- Effects on water chemistry as a result of surface area and sample preparation;
- Changes in the chemistry of the reacting phases;
- Distribution and nature of secondary phases.

These studies are similar in design to earlier studies that focused on the Bullfrog Member of the Crater Flat Tuff (Oversby and Knauss, 1983;

Knauss, 1984a), which also used the Teflon-lined static autoclaves.

We report here the quantitative analyses of both aqueous and solid phases resulting from the hydrothermal interaction of polished wafers of Topopah Spring tuff with a natural ground water. The experiments were run for up to 120 days at 150°C both with the tuff fully submerged and with the tuff exposed to water-saturated air. They were also run before the completion of a hydrothermal experimental facility containing Dickson-type gold-cell rocking autoclaves, and must be considered preliminary. Subsequent rock/water interaction experiments have been run using the rocking autoclaves (13 completed and 4 in progress), and some of the results are either already published (Knauss et al., 1983) or have been submitted for publication (Knauss et al., 1984). A comparison of analogous experiments using the two different experimental techniques shows that most, but not all, of the aqueous phase results are similar. The solid phase results compare less favorably. Any data or interpretations from the experiments in the static, Teflon-lined autoclaves that disagree with the subsequent gold-cell rocking-autoclave experiments are so noted.

Sample Preparation and Characterization

The tuff used in these experiments was collected in outcrop from a location that exposed Topopah Spring Member tuff (Tpt) stratigraphically equivalent to that within the proposed repository interval beneath Yucca Mountain (Knauss, 1984b). The initial steps used to prepare the material are described in the aforementioned text. Cores 1 in. in diameter were drilled with a water-lubricated diamond corer and sliced into 0.1-in.-thick wafers using an Isomet saw with a 0.012-in.-thick low-concentration diamond blade, lubricated with a water-plus-water-soluble oil mixture. Both sides of each wafer were then rough-ground with 10-micron aluminum oxide and polished optically flat with 1.0-micron and finally 0.3-micron aluminum oxide. In this respect they differ slightly from the wafers of Bullfrog Member tuff prepared in the earlier experiments (Knauss, 1984a), which were only fine-polished on one side. The polished wafers were washed repeatedly in distilled water and cleaned in an ultrasonic bath to remove any adhering aluminum oxide.

The water used in the experiments was collected from well J-13, which is the reference water for the NNWSI program. This natural water is collected in large quantities from a producing horizon within a highly fractured interval in the Tpt unit. The water is neither filtered nor acidified. It is stored in plastic-lined, 55-gal drums, and water from only one sample time is used in any given experiment. The water, however, is periodically discarded and replaced with a new supply.

The characterization work that was done on the Tpt tuff used in all Waste Package experimental work is described in some detail in Knauss, 1984b. The reader is referred to this document, which presents results of petrographic examination, as well as analysis by XRD, NAA, and SEM/EMP using both wavelength-dispersive (WDS) and energy-dispersive (EDS) techniques. Especially pertinent here are the EMP analyses presented in that report for wafers designated Tpt FR CW0a and CW0c which are two unreacted wafers subjected to the same types of analyses made on the reacted wafers to be presented here.

Not presented in the characterization report are the specific surface area measurements made on the polished wafers. We measured the gas adsorption (BET) surface areas of two representative wafers using argon gas and a 5-point fitted curve to the data. The results follow:

Sample	Surface area (m^2/g)
A	0.367
B	0.389
Average	0.378 ± 0.016

Note that this specific surface area for the polished wafers is approximately three times smaller than the specific surface area measured for the crushed Tpt tuff (1.15 ± 0.29 m^2/g; Knauss, 1984b). Similar comparisons made for the Bullfrog Member tuff show much smaller differences, and attest to a high interconnected porosity for the Bullfrog. The measured gas adsorption surface areas (nominally 0.907 m^2) are much higher than the geometric surface areas calculated from the dimensions of the wafer (nominally 0.0012 m^2).

Experimental Techniques

The general experimental plan was nearly identical to that used in the earlier Bullfrog Member tuff static hydrothermal experiments (Knauss, 1984a). The key elements were to:

- Characterize the starting materials.
- React the polished Tpt wafer with J-13 water at 150°C, either fully submerged or exposed to water-saturated air with enough excess water present to allow refluxing.
- Vary the reaction time to span 120 days with quenched samples taken at specific time intervals.
- Analyze filtered, acidified solutions for cations.
- Analyze filtered, unacidified solutions for anions.
- Measure pH electrochemically on unfiltered solutions.
- Determine weight changes in wafers.
- Characterize solid phases (primary and secondary) by SEM observation and EMP analysis.

Figure 2 in Knauss (1984a) shows that the wafers could be supported on the Teflon blocks with platinum pins in such a way as to expose the entire surface area to the solution and/or refluxing fluid. The average weight of the polished wafers was about 2.4 g, so the surface area (as measured by BET) exposed to reaction was on the order of 0.907 m^2. This falls within the range of surface areas covered in the analogous experiments with crushed tuff (Oversby, 1984).

In the fully submerged experiments approximately 80 g of J-13 water were used, while in the water-saturated air experiments 35 g of J-13 water were used.

The cleaning procedure used for the Teflon-lined autoclaves, as well as a description of the sampling procedure used, are provided in Knauss (1984a). The analytical methods and operating conditions used for cation analysis (ICP-ES), anion analysis (IC), and EMP analysis are also the same as those detailed in this earlier report. The following sample code is used in the discussion of the aqueous and solid phase analytical results:

Time (days)	Submerged	Water-saturated air
14	CW1	CW5
28	CW2	CW6
56	CW3	CW7
112	CW4	CW8

Results of Aqueous Phase Analyses

Table 1 contains the results of the ICP cation analyses, the quenched (25°C) pH, and the wafer weight loss. The anion analyses are presented in Table 2. These data have also been plotted vs reaction time and are presented in Figs. 1 through 9.

The trends in the solution chemistry data for the fully submerged wafers are reviewed here, and show an initial increase in both aluminum and potassium followed by a regular decrease approaching a steady-state value. The calcium was removed from solution exponentially to a steady-state value, while magnesium and iron were effectively removed very rapidly from solution. The silicon rose asymptotically to a value slightly

Table 1. ICP cation results for Tpt wafers.

Sample no.	Mass (g)	Element (ppm)									Wt loss (%)
		Al	B	Fe	Si	Ca	K	Mg	Na	pH	
J-13	0	0.012	0.122	0.006	27.0	12.5	5.1	1.91	43.6	7.56	0
1	2.9227	0.537	0.207	0.003	87.2	4.14	11.9	0.028	46.5	7.52	1.16
2	2.3026	0.442	0.202	0.010	102.	3.84	9.04	0.047	47.5	8.06	1.38
3	2.4998	0.367	0.257	0.000	119.	3.36	8.31	0.010	47.6	8.51	1.40
4	2.3338	0.358	0.309	0.000	132.	4.24	7.12	0.007	61.0	8.70	1.44
5	2.5565	0.000	0.605	0.050	25.2	7.10	4.85	0.292	44.3	7.33	0.09
6	2.6755	0.000	0.495	0.000	28.5	6.27	7.56	0.258	49.7	7.35	0.11
7	2.6233	0.024	0.356	0.003	27.7	5.68	6.37	0.174	48.9	7.40	0.10
8	2.3751	0.000	0.334	0.000	35.7	6.16	6.96	0.040	58.5	8.50	0.12
Detection limit	0	0.008	0.004	0.003	0.008	0.012	0.16	0.003	0.002	0	0

Table 2. IC results for Tpt wafers.

Tpt	Element (ppm)					
	F	Cl	NO_2	NO_3	SO_4^{2}	$C_2O_4^{2}$
J-13	2.3	6.8	—[a]	9.2	18.8	0
1	3.5	8.3	0.3	10.6	19.4	1.2
2	3.5	8.1	0.3	10.5	19.3	1.1
3	3.3	8.4	0.5	10.9	19.3	3.8
4	3.8	8.6	0.6	12.2	21.0	2.5
5	4.7	7.2	1.2	9.9	18.4	2.1
6	5.5	9.9	1.6	14.1	18.8	2.1
7	9.2	8.9	2.7	12.8	18.5	0.6
8	7.8	9.6	5.6	16.0	21.5	2.1

[a] Not measured.

higher than, but not inconsistent with, cristobalite saturation. The quench pH increased steadily during the experiments, reaching a value of 8.70 after 112 days. The sodium, boron, and all anions showed a step increase as a result of the presence of a component of readily soluble material in the outcrop material used in these experiments. This effect was noted by Oversby and Knauss (1983) in earlier experiments using outcrop samples of Bullfrog Member tuff. The necessity for establishing baseline values for dissolved species in rock/water interaction experiments using outcrop samples was provided in Knauss (1984b). Mass balance estimates made from changes in solution composition show that the weight loss observed in the wafers is consistent with dissolution of both cristobalite and alkali feldspar (as the dominant

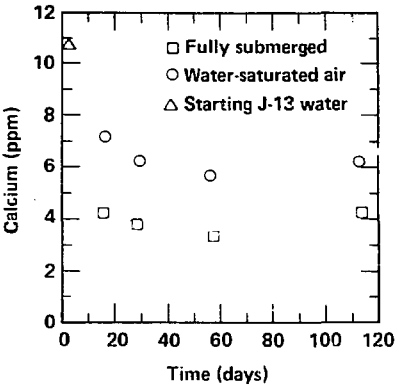

Figure 2. Aqueous calcium concentrations in the Tpt wafer experiments.

silicon sources) as well as the dissolution of a small, readily soluble fraction of evaporite minerals.

The solution chemistry for the water-saturated air experiments showed the following trends. Aluminum, iron, and magnesium immediately decreased to very low levels. The calcium decreased more rapidly and to lower levels than in the submerged experiments. Both boron and potassium increased to values that by the end of the experiment were nearly identical to those reached at the conclusion of the fully submerged experiments.

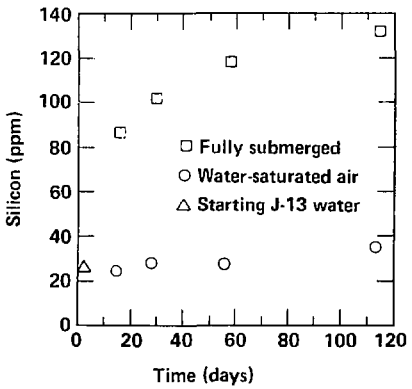

Figure 1. Aqueous silicon concentrations in the Tpt wafer experiments.

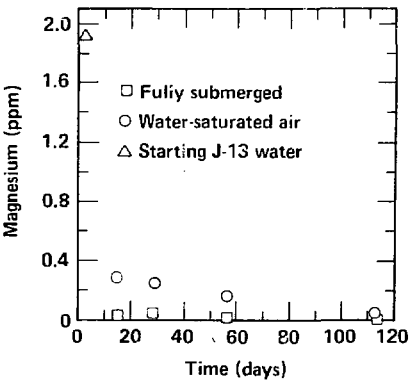

Figure 3. Aqueous magnesium concentrations in the Tpt wafer experiments.

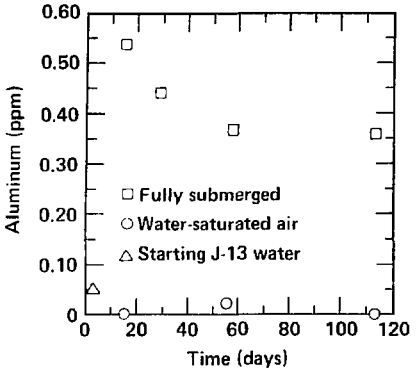

Figure 4. Aqueous aluminum concentrations in the Tpt wafer experiments.

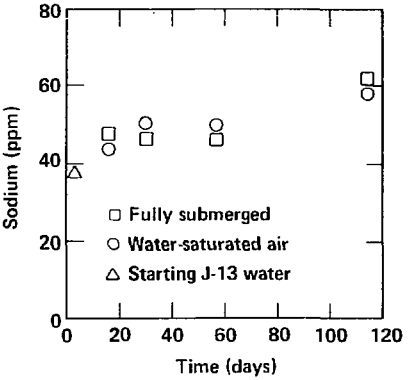

Figure 6. Aqueous sodium concentrations in the Tpt wafer experiments.

The sodium concentrations were similar for submerged and refluxed samples, whereas the anion concentrations were either similar or slightly higher for the refluxed samples. The silicon increased only very slightly and only in the experiment with the longest reaction time, indicating some limited dissolution. As with the submerged samples, the quench pH rose with time (although not as regularly as for the submerged samples), and reached a value of 8.50 in the longest experiment. A uniform and low weight loss was observed in the wafers.

The agreement between the solution compositions seen in the submerged wafer experiments and similar experiments run using crushed tuff (Oversby, 1984) is reasonably good. The main differences between the experiments were in aluminum and silicon concentrations. The crushed tuff experiments resulted in somewhat higher aluminum concentrations and slightly lower silicon

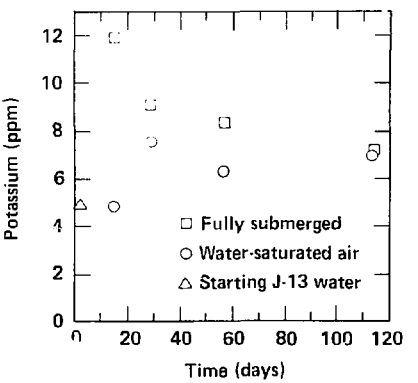

Figure 5. Aqueous potassium concentrations in the Tpt wafer experiments.

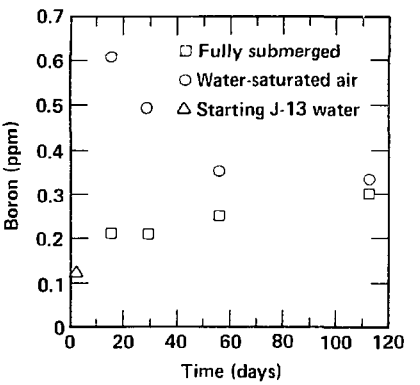

Figure 7. Aqueous boron concentrations in the Tpt wafer experiments.

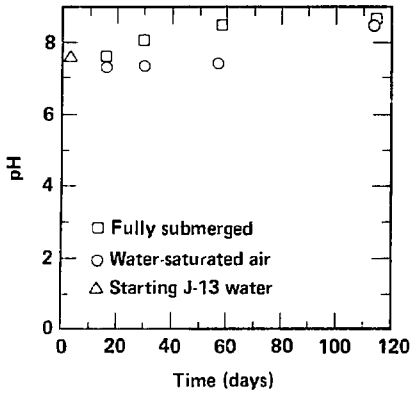

Figure 8. Measured quench pH in the Tpt wafer experiments.

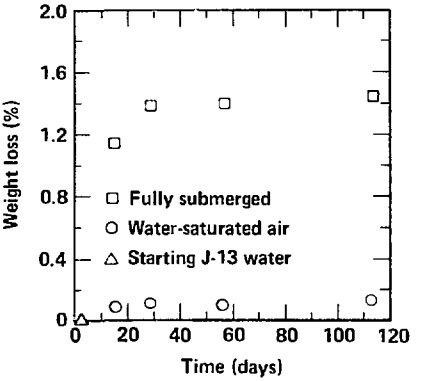

Figure 9. Measured net weight loss in the Tpt wafers.

concentrations. Note that the crushed tuff experiments were run in small Teflon-lined autoclaves that were rolled continuously during the experiment, whereas the wafer experiments were not agitated. The solution results for other constituents were quite similar.

As was noted earlier, these preliminary experiments were conducted before the Dickson-type gold-cell rocking autoclaves were installed. Problems encountered with the Teflon-lined autoclaves have been reported previously (Knauss et al., 1983; Oversby, 1984). Briefly, these include degassing of volatiles throughout the course of the experiment and quenching effects during the act of sampling.

The effect of degassing volatiles in this system (Tpt plus J-13) is primarily CO_2 loss and the resulting continuous decrease in alkalinity and increase in pH with reaction time. Although the alkalinity was not measured during these preliminary experiments, subsequent experiments that measured alkalinity using the Teflon-lined autoclaves found that the decrease in alkalinity as a function of reaction time was due to degassing of carbon dioxide (Oversby, 1984). Both the fully submerged and water-saturated air experiments clearly show an increase in pH due to this effect. The speciation of dissolved constituents that are a function of pH might also be affected to some degree. For example, the slightly elevated silicon concentration (above that expected for saturation with respect to cristobalite) might be due to the presence of significant $H_3SiO_4^-$ anion. This explanation can account for the measured silicon at day 120 being 8% higher than cristobalite solubility, since the measured pH was 8.7. At quench pH 8.7 (equivalent to an *in-situ* pH 7.8) the dissolved silicon concentration determined by saturation with cristobalite is some 6% higher at 150°C than one would calculate at a lower pH (say, less than 7.5) where SiO_2 is the only species present (Wolery, 1984).

As for quenching effects, the only way they can be evaluated is by comparing these results with those obtained from analogous experiments using the Dickson-type gold-cell rocking autoclaves that were specifically designed to allow sampling at *in-situ* conditions during the course of the experiment.

The results of the specific rocking autoclave experiments that are analogous to those reported here will be published in a later report (Knauss et al., 1984). The following comparison is made. For silicon the results were quite similar over 64 days, the length of the rocking autoclave experiment. For calcium the trends were identical, but the Teflon-lined autoclaves produced a steady-state value (6 ppm) slightly lower than the rocking autoclaves (7–8 ppm). The rapid removal of magnesium from solution was observed in both cases, although it was more rapid in the rocking autoclave experiments. The trend for aluminum was

also identical, although the maximum concentration (1.5 ppm) and steady-state value (0.5 ppm) achieved in the rocking autoclave experiments were both higher than those in the Teflon-lined autoclaves (0.55 and 0.35 ppm). Note that the first sample taken in the Teflon-lined experiments was at day 14; at day 16 in the rocking autoclave the aluminum value was 1.0 ppm. In the Teflon-lined experiments we are clearly past the peak aluminum value before the first sample. Also, the higher rocking autoclave values may be partly due to agitation during reaction. Results for crushed tuff reacted in rolled Teflon-lined vessels have a peak concentration of 2.7 ppm decreasing to 1.1 ppm by day 48 at 150°C (Oversby, 1984). The trends for potassium were again consistent, but the Teflon-lined autoclave values were considerably higher during the initial pulse and then decreased to a steady-state value comparable to the rocking autoclave value. With the exception of the last point at 120 days (which is high), the sodium data for the Teflon-lined autoclaves were quite similar to the data obtained with the rocking autoclaves. As mentioned above, the pH increased with reaction time in the Teflon-lined autoclaves to a maximum value of 8.70, whereas in the rocking autoclave experiments the quench pH dropped to approximately 6.8 and remained quite constant. The anion content of the Teflon-lined autoclave experiments tended to be higher than the anion content observed in the rocking autoclave experiments. To some extent this can be explained by dissolution of a residual evaporite mineral phase (surviving the washing provided by core cutting and polishing) into a smaller volume of fluid. The Teflon-lined autoclaves were run with 80 g of J-13 water, whereas the rocking autoclave experiments were run with about 200 g of J-13 water.

Overall, there are measurable differences in at least some of the aqueous measurements made, but they are relatively minor. All of the differences seen (alkalinity, pH, and possibly calcium) can be attributed to the degassing of volatiles through the Teflon-lined vessels. The minimization of quenching effects in the Teflon-lined autoclave experiments is a direct result of the extreme effort made to sample the bombs as rapidly as possible upon cooling and the immediate separation of the wafer from the fluid phase. Quenching effects on the solid phase are dealt with in the following section.

Results of Solid Phase Analyses

The solid phase analysis generally followed the scheme outlined in Knauss (1983). The carbon-coated reacted wafers were examined using the scanning electron microscope (SEM) at both low and high magnification to locate phenocrysts for quantitative WDS analysis and to locate small secondary phases for semiquantitative EDS analysis.

The quantitative WDS analysis of primary phases present in wafers CW2, CW3, CW4, CW7, and CW8 is presented in Tables 3 through 7, respectively. For a comparison with unreacted wafers, the reader is referred to Tables 4 and 5 in Knauss (1984b). Note that all iron is calculated as FeO and in minerals with high Fe^{+3}/Fe^{+2} ratios, apparently low oxide totals will result. Because what appeared to be a real difference was observed in the mean composition of the plagioclase feldspars in the Bullfrog tuff hydrothermal experiments (Knauss, 1984a), the calculated end-member compositions of the plagioclase feldspar phenocrysts in wafers CW3, CW4, and CW8 are also presented as histograms in Figs. 10 through 12, respectively. For comparison, the reader should refer to Fig. 30 in Knauss (1984b), which shows a bimodal distribution with a main peak at 17 mol% anorthite and a minor peak at 40 mol % anorthite. Although not presented here, histograms were also made for the data from each wafer on the calculated end-member compositions of the alkali feldspar phenocrysts and on the Mg/Mg + Fe ratio in the biotite phenocrysts. These plots were all made to more easily recognize compositional changes in the major phases present in the wafers as a function of the extent of hydrothermal reaction. The following observations can be made with regard to these reacted wafers:

1. In the submerged experiments, most of the phenocrysts displayed minor dissolution features such as micron-sized etch pits on their surfaces as a result of reaction. These suggest a surface-reaction-controlled dissolution mechanism.

2. As seen in the histograms, the calculated anorthite end-member composition of the plagioclase feldspar phenocrysts was unchanged by 4 months of reaction with J-13 water at 150°C. This

Table 3. Microprobe analyses for sample Tpt CW2. The identification Ph X Pt Y refers to the original SEM photo number (X) and the specific point on that photo (Y) that was analyzed by quanititative WDS.

	Sanidine											
Oxide	Ph10 Pt1	Ph10 Pt2	Ph10 Ph3	Ph10 Pt4	Ph10 Pt5	Ph18 Pt1	Ph18 Pt2	Ph18 Pt3	Ph18 Pt4	Ph25 Pt1	Ph25 Pt2	Ph25 Pt3
SiO_2	66.02	66.07	65.97	68.73	66.71	64.88	65.88	66.07	65.93	66.65	65.82	68.15
Al_2O_3	18.39	18.46	18.03	18.25	18.14	19.44	18.89	19.43	19.07	19.61	18.93	19.02
K_2O	9.82	10.45	10.16	10.38	10.29	9.72	9.80	9.37	9.48	9.66	10.11	9.98
Na_2O	3.95	3.84	3.80	4.21	3.96	4.77	4.76	4.82	4.82	4.60	4.37	4.35
CaO	0.11	0.11	0.11	0.17	0.11	0.36	0.36	0.36	0.36	0.17	0.17	0.17
MgO	0.10	0.02	0.04	0.06	0.05	0.05	0.03	0.03	0.03	0.08	0.09	0.09
TiO_2	0.00	0.03	0.06	0.12	0.12	0.00	0.00	0.05	0.03	0.00	0.00	0.00
FeO	0.49	0.09	0.32	0.08	0.13	0.17	0.18	0.19	0.14	0 09	0.13	0.09
BaO	0.04	0.04	0.07	0.10	0.00	0.00	0.00	0.00	0.00	0.00	0.00	0.00
Total	98.92	99.11	98.50	102.11	99.51	99.39	99.90	100.32	99.85	100.85	99.63	101.84
Qz	–	–	–	–	–	–	–	–	–	–	–	–
Or	61.79	63.92	63.49	61.38	62.75	57.15	57.44	55.99	55.48	57.99	60.30	59.70
Ab	37.92	35.79	36.15	37.77	36.66	42.67	42.38	43.83	42.76	41.91	39.61	39.44
An	0.29	0.29	0.36	0.84	0.58	0.18	0.18	0.18	1.76	0.10	0.09	0.86

	Sanidine												
Oxide	Ph26 Pt1	Ph26 Pt2	Ph26 Ph3	Ph45 Pt1	Ph45 Pt2	Ph45 Pt3	Ph45 Pt4	Ph46 Pt1	Ph46 Pt2	Ph46 Pt3	Ph47 Pt1	Ph47 Pt2	Ph47 Pt3	Ph47 Pt4
SiO_2	65.89	65.87	66.75	68.61	66.89	67.32	65.45	67.54	68.28	67.68	66.96	67.68	68.87	67.19
Al_2O_3	18.82	19.22	18.65	19.08	18.70	18.62	18.10	18.67	19.07	18.56	19.10	19.02	19.08	18.98
K_2O	9.33	9.07	9.46	9.54	10.33	10.94	9.86	10.70	9.77	9.92	10.06	10.17	9.93	9.95
Na_2O	4.76	5.01	4.66	4.27	3.83	3.20	4.00	3.81	4.17	4.36	4.18	4.21	4.16	3.40
CaO	0.23	0.23	0.23	0.13	0.13	0.13	0.13	0.19	0.19	0.19	0.10	0.10	0.10	0.10
MgO	0.03	0.05	0.03	0.06	0.10	0.10	0.05	0.13	0.04	0.09	0.02	0.10	0.01	0.00
TiO_2	0.00	0.06	0.00	0.04	0.00	0.03	0.13	0.00	0.00	0.11	0.00	0.00	0.00	0.01
FeO	0.19	0.30	0.21	0.34	0.21	0.20	1.12	0.08	0.05	0.44	0.00	0.03	0.02	0.06
BaO	0.00	0.00	0.82	0.08	0.60	0.00	0.00	0.00	0.00	0.00	0.00	0.00	0.00	0.07
Total	99.25	99.81	100.81	102.15	100.20	100.54	98.85	101.17	101.58	101.35	101.43	101.30	102.18	99.75
Qz	–	–	–	–	–	–	–	–	–	–	–	–	–	–
Or	56.27	54.31	56.58	59.21	63.65	68.90	61.50	64.46	60.24	59.44	61.10	61.19	60.88	65.55
Ab	43.62	45.57	42.27	40.44	36.00	30.75	37.80	35.07	39.29	39.63	38.63	38.54	38.85	33.92
An	0.11	0.12	1.15	0.35	0.35	0.25	0.70	0.47	0.47	0.93	0.27	0.27	0.27	0.54

Table 3. (Continued)

	Sanidine									Plagioclase		
Oxide	Ph48 Pt1	Ph48 Pt2	Ph49 Pt1	Ph49 Pt2	Ph49 Pt3	Ph50 Pt1	Ph51 Pt1	Ph51 Pt2	Ph51 Pt3	Ph16 Pt1	Ph16 Pt2	Ph16 Pt3
SiO_2	67.46	68.99	67.72	69.31	68.27	68.84	67.13	68.50	66.88	66.37	66.90	67.03
Al_2O_3	18.69	19.15	18.67	18.72	18.76	18.93	18.73	18.30	18.39	22.84	22.02	22.59
K_2O	10.74	10.46	10.71	10.03	11.01	9.78	10.06	10.53	9.91	1.39	1.80	1.45
Na_2O	3.77	4.14	3.55	3.71	3.52	4.07	4.43	4.10	4.22	8.43	9.21	8.09
CaO	0.05	0.09	0.10	0.12	0.06	0.17	0.17	0.06	0.18	2.90	2.51	2.80
MgO	0.02	0.02	0.00	0.00	0.02	0.00	0.00	0.01	0.20	0.02	0.04	0.05
TiO_2	0.03	0.03	0.07	0.03	0.06	0.09	0.09	0.15	0.16	0.04	0.00	0.06
FeO	0.07	0.08	0.09	0.04	0.05	0.33	0.11	0.05	0.49	0.21	0.28	0.30
BaO	0.07	0.04	0.11	0.15	0.15	0.00	0.00	0.00	0.00	0.11	0.10	0.00
Total	100.89	103.02	101.01	102.10	101.90	102.21	100.72	101.70	100.42	102.41	102.85	102.31
Qz	–	–	–	–	–	–	–	–	–	–	–	–
Or	65.10	62.19	66.19	63.68	67.13	60.77	59.49	62.73	60.19	8.90	10.06	9.04
Ab	34.66	37.34	33.29	35.70	32.54	38.34	39.67	36.98	38.89	76.55	78.16	76.33
An	0.25	0.47	0.52	0.62	0.33	0.89	0.84	0.30	0.93	14.55	11.78	14.64

	Plagioclase						Magnetite				
Oxide	Ph52 Pt1	Ph52 Pt2	Ph54 Pt1	Ph54 Pt2	Ph55 Pt1	Ph55 Pt2	Oxide	Ph29 Pt1	Ph29 Pt2	Ph42 Pt1	Ph42 Pt2
SiO	65.46	64.71	65.45	64.67	63.37	61.51	SiO_2	0.68	1.69	0.00	0.00
Al_2O_3	23.25	22.96	23.44	23.46	24.96	25.90	Al_2O_3	1.05	0.015	0.69	0.56
K_2O	1.19	1.28	1.30	1.10	0.65	0.56	K_2O	–	–	–	–
Na_2O	8.93	8.82	8.76	8.60	8.20	7.64	Na_2O	–	–	–	–
CaO	3.61	3.46	3.63	3.93	5.42	6.53	CaO	–	–	–	–
MgO	0.04	0.06	0.04	0.05	0.06	0.05	FeO	85.40	81.92	86.82	84.73
TiO_2	0.06	0.00	0.03	0.00	0.09	0.11	MgO	0.43	0.38	0.03	0.16
FeO	0.15	0.16	0.13	0.11	0.26	0.22	MnO	1.53	1.58	1.51	1.75
BaO	0.10	0.00	0.12	0.00	0.18	0.13	TiO_2	1.76	2.40	1.70	4.25
							F	–	–	–	–
							Cl	–	–	–	–
Total	102.78	101.45	102.89	101.92	103.18	102.66	Total	89.84	90.02	90.76	91.46
Qz	–	–	–	–	–	–	Ti/Fe	0.019	0.026	0.018	0.045
Or	6.70	7.28	7.37	6.30	3.70	3.17	Mg/Mg + Fe	0.009	0.008	0.001	0.003
Ab	76.24	76.19	75.34	74.78	70.50	65.72	Ulvospinel	0.028	0.048	0.026	0.101
An	17.06	16.53	17.29	18.92	25.80	31.11	Magnetite	0.972	0.952	0.974	0.899

Table 3. (Continued)

	Ilmenite						Biotite							
Oxide	Ph29 Pt1	Ph29 Pt2	Ph40 Pt1	Ph40 Pt2	Ph40 Pt3	Oxide	Ph32 Pt1	Ph32 Pt2	Ph32 Pt3	Ph32 Pt4	Ph35 Pt1	Ph35 Pt2	Ph35 Pt3	Ph35 Pt4
SiO_2	0.57	0.29	0.00	0.11	0.00	SiO_2	36.35	37.6[illegible]	33.31	37.92	36.65	34.94	37.22	37.16
Al_2O_3	0.22	0.15	–	0.07	–	Al_2O_3	13.23	12.91	11.69	13.90	13.44	12.89	13.61	13.28
K_2O	–	–	–	–	–	K_2O	8.23	8.37	7.69	8.82	8.17	8.08	8.53	8.61
Na_2O	–	–	–	–	–	Na_2O	0.50	0.42	0.39	0.45	0.50	0.45	0.46	0.47
CaO	–	–	–	–	–	CaO	0.12	0.12	0.25	0.12	0.17	0.17	0.17	0.17
FeO	46.18	54.93	43.24	43.18	43.85	FeO	21.03	17.91	21.07	18.20	20.96	25.50	21.27	20.22
MgO	0.81	0.61	0.00	0.15	0.00	MgO	11.42	12.18	11.05	11.48	10.76	10.98	11.55	10.86
MnO	12.28	5.77	0.99	1.01	0.96	MnO	1.24	1.14	1.33	1.12	0.73	0.78	0.72	0.75
TiO_2	42.89	31.97	48.73	50.17	48.99	TiO_2	3.97	3.51	3.96	4.21	4.68	3.89	3.63	4.29
F	–	–	–	–	–	F	0.00	0.00	0.00	1.39	0.00	0.05	0.00	0.04
Cl	–	–	–	–	–	Cl	0.20	0.00	0.00	0.03	0.00	0.00	0.00	0.00
Total	96.95	93.72	92.68	94.69	93.79	Total	96.08	94.24	90.76	97.60	96.07	97.74	97.17	95.85
Ti/Fe	0.960	0.523	1.014	1.045	1.005	Ti/Fe	0.170	0.176	0.169	0.208	0.201	0.137	0.154	0.191
Mg/Mg + Fe	0.035	0.020	0.000	0.006	0.000	Mg/Mg + Fe	0.494	0.550	0.486	0.532	0.480	0.437	0.494	0.492
Ilmenite	0.773	0.582	0.996	1.008	0.992									
Hematite	0.227	0.418	0.004	0.008	0.008									

	Biotite										Matrix	
Oxide	Ph36 Pt1	Ph36 Pt2	Ph36 Pt3	Ph36 Pt4	Ph37 Pt1	Ph37 Pt2	Ph37 Pt3	Ph37 Pt4	Ph37 Pt5	Ph37 Pt6	Oxide	Ph60 Pt1	Ph61 Pt1
SiC_2	36.60	36.79	37.15	37.31	35.53	[illegible]	35.63	36.78	36.10	36.90	SiO_2	77.43	81.15
Al_2O_3	13.01	12.93	13.19	13.53	14.52	14.46	14.84	14.84	13.96	14.53	Al_2O_3	13.43	11.07
K_2O	7.83	8.07	8.09	8.60	7.99	8.14	7.92	8.09	8.06	8.09	K_2O	6.34	4.33
Na_2O	0.49	0.49	0.47	0.49	0.38	0.48	0.49	0.41	0.27	0.45	Na_2O	3.10	3.42
CaO	0.15	0.15	0.12	0.15	0.18	0.18	0.18	0.18	0.23	0.18	CaO	0.34	0.36
FeO	21.95	22.27	22.48	20.37	18.94	18.59	17.20	18.41	17.96	17.87	MgO	0.09	0.13
MgO	11.70	11.88	11.84	11.61	9.86	9.99	9.34	9.77	8.49	9.68	FeO	0.25	0.22
MnO	0.81	0.68	0.76	0.65	1.05	1.13	2.62	1.05	1.19	1.08	TiO_2	0.01	0.00
TiO_2	4.32	4.12	3.45	4.27	4.53	4.64	4.65	4.50	4.57	4.73	MnO	0.02	0.04
F	0.00	0.00	0.00	0.00	0.00	0.00	0.00	0.00	0.00	0.00	BaO	0.00	0.00
Cl	0.00	0.00	0.00	0.00	0.00	0.00	0.00	0.00	0.00	0.00			
Total	96.86	97.37	98.59	95.99	92.30	94.79	92.87	94.03	90.82	93.51	Total	101.03	100.73
Ti/Fe	0.177	0.166	0.178	0.198	0.215	0.225	0.243	0.220	0.229	0.238	Qz	32.19	41.09
Mg/Mg + Fe	0.490	0.490	0.487	0.519	0.484	0.492	0.494	0.488	0.460	0.494	Or	38.14	26.03
											Ab	28.30	31.18
											An	1.37	1.70

Table 4. Microprobe analyses for sample Tpt CW3.

	Sanidine														
Oxide	Ph3 Pt2	Ph4 Pt1	Ph4 Pt2	Ph5 Pt1	Ph5 Pt2	Ph7 Pt1	Ph7 Pt2	Ph10 Pt1	Ph10 Pt2	Ph12 Pt1	Ph12 Pt2	Ph13 Pt1	Ph13 Pt2	Ph15 Pt1	Ph15 Pt2
SiO_2	66.70	65.97	65.51	66.64	66.84	65.94	67.06	67.31	66.91	67.80	67.50	65.73	64.63	65.17	66.51
Al_2O_3	18.29	19.07	19.30	17.95	18.26	19.20	18.19	19.37	19.85	18.29	18.73	19.68	19.30	18.85	18.30
K_2O	11.50	8.79	9.43	10.37	10.17	9.80	10.83	9.42	9.54	10.44	10.64	9.76	9.42	10.06	10.47
Na_2O	3.29	5.06	4.78	4.05	3.91	4.42	3.75	4.82	4.62	3.66	3.86	4.39	4.71	4.05	3.73
CaO	0.11	0.39	0.35	0.08	0.08	0.20	0.13	0.24	0.23	0.08	0.15	0.34	0.42	0.19	0.10
MgO	0.01	0.05	0.03	0.04	0.05	0.00	0.07	0.06	0.03	0.03	0.06	0.03	0.03	0.04	0.02
TiO_2	0.00	0.02	0.00	0.41	0.02	0.00	0.00	0.00	0.04	0.02	0.00	0.00	0.00	0.01	0.02
FeO	0.18	0.19	0.18	0.15	0.17	0.10	0.15	0.19	0.13	0.15	0.11	0.18	0.15	0.15	0.15
BaO	0.00	0.00	0.13	0.00	0.13	0.00	0.10	0.00	0.00	0.00	0.00	0.07	0.14	0.06	0.00
Total	100.08	99.53	100.72	99.70	99.62	99.66	100.28	101.40	101.34	100.48	101.05	100.18	98.82	98.58	99.30
Qz	–	–	–	–	–	–	–	–	–	–	–	–	–	–	–
Or	69.37	52.36	55.54	62.52	62.88	58.81	65.14	55.61	57.02	64.98	64.05	58.46	55.69	61.50	64.61
Ab	30.06	45.71	42.73	37.05	36.69	40.28	34.22	43.18	41.83	34.59	35.21	39.85	42.23	37.51	34.89
An	0.58	1.93	1.73	0.42	0.42	1.02	0.64	1.21	1.16	0.43	0.74	1.69	2.08	0.99	0.50

	Sanidine										Plagioclase			
Oxide	Ph16 Pt1	Ph16 Pt2	Ph23 Pt1	Ph23 Pt2	Ph24 Pt1	Ph24 Pt2	Ph28 Pt1	Ph28 Pt2	Ph29 Pt1	Ph29 Pt2	Ph14 Pt1	Ph14 Pt2	Ph18 Pt1	Ph14 Pt2
SiO_2	67.14	67.93	66.95	66.21	66.12	66.28	66.29	65.51	64.89	65.82	63.17	62.35	63.46	63.06
Al_2O_3	17.85	18.60	18.63	19.11	19.36	20.02	19.38	19.12	19.40	19.35	22.51	22.51	23.10	23.03
K_2O	10.37	9.78	10.19	8.56	10.27	9.79	9.83	9.76	10.41	10.84	1.30	1.18	0.90	0.82
Na_2O	3.49	4.09	4.02	5.44	4.13	4.56	4.74	4.67	4.19	4.97	8.67	8.47	8.86	8.58
CaO	0.10	0.25	0.27	0.54	0.29	0.36	0.32	0.30	0.27	0.22	3.34	3.53	3.85	3.88
MgO	0.03	0.07	0.02	0.02	0.03	0.02	0.03	0.04	0.03	0.01	0.03	0.03	0.00	0.00
TiO_2	0.09	0.06	0.01	0.50	0.08	0.07	0.04	0.04	0.06	0.11	0.04	0.00	0.00	0.05
FeO	0.19	0.53	0.20	0.16	0.00	0.13	0.12	0.16	0.12	0.11	0.13	0.18	0.26	0.32
BaO	0.04	0.00	0.00	0.00	0.15	0.00	0.00	0.59	0.00	0.30	0.00	0.00	0.00	0.00
Total	99.30	101.31	100.29	100.54	100.45	101.23	100.74	100.19	99.38	100.84	99.19	98.25	100.44	99.74
Qz	–	–	–	–	–	–	–	–	–	–	–	–	–	–
Or	65.88	60.44	61.71	49.59	61.23	57.59	56.89	57.08	61.25	63.05	7.52	6.95	5.13	4.79
Ab	33.61	38.28	36.89	47.77	37.32	40.61	41.57	41.44	37.40	35.88	76.21	75.61	76.45	76.14
An	0.51	1.28	1.39	2.64	1.46	1.80	1.54	1.47	1.35	1.07	16.27	17.45	18.42	19.07

	Plagioclase							Ilmenite					
Oxide	Ph19 Pt1	Ph19 Pt2	Ph22 Pt1	Ph22 Pt2	Ph27 Pt1	Ph27 Pt2	Ph27 Pt3	Oxide	Ph32 Pt1	Ph32 Pt2	Ph33 Pt1	Ph33 Pt2	Ph39 Pt1
SiO_2	64.23	64.10	63.66	64.04	65.28	64.23	65.28	SiO_2	0.03	0.24	0.18	0.09	0.04
Al_2O_3	22.44	22.60	22.74	21.86	22.28	22.09	22.88	Al_2O_3	0.07	0.19	0.05	0.00	0.09
K_2O	1.26	1.16	1.08	1.28	1.28	1.44	1.18	K_2O	–	–	–	–	–
Na_2O	8.69	8.61	8.92	8.69	8.71	8.64	8.59	Na_2O	–	–	–	–	–
CaO	3.33	3.38	3.35	3.10	3.29	3.11	3.46	CaO	–	–	–	–	–
MgO	0.02	0.00	0.00	0.00	0.02	0.02	0.00	FeO	45.71	45.38	40.78	46.22	46.13
TiO_2	0.00	0.00	0.00	0.00	0.00	0.06	0.00	MgO	0.22	0.41	0.09	0.18	0.23
FeO	0.17	0.23	0.17	0.18	0.14	0.14	0.13	MnO	4.33	4.04	1.77	4.13	3.34
BaO	0.00	0.00	0.00	0.00	0.00	0.00	0.00	TiO_2	49.38	46.73	47.18	41.92	47.54
								F	–	–	–	–	–
								Cl	–	–	–	–	–
Total	100.14	100.09	99.91	99.16	101.00	99.67	101.52	Total	99.74	96.99	90.05	92.54	97.36
Qz	–	–	–	–	–	–	–	Ti/Fe	0.972	0.926	1.041	0.816	0.927
Or	7.34	6.79	6.19	7.50	7.39	8.41	6.91	Mg/Mg+Fe	0.009	0.016	0.004	0.007	0.009
Ab	76.46	76.56	77.65	77.27	76.60	76.40	76.14	Ilmenite	0.930	0.903	0.997	0.838	0.917
An	16.20	16.65	16.15	15.24	16.01	15.19	16.95	Hematite	0.070	0.097	0.003	0.162	0.083

Table 4. (Continued)

	Magnetite						Biotite						
Oxide	Ph21 Pt1	Ph21 Pt2	Ph30 Pt1	Ph30 Pt2	Ph32 Pt1	Ph32 Pt2	Ph17 Pt1	Ph17 Pt2	Ph18 Pt1	Ph18 Pt2	Ph25 Pt1	Ph25 Pt2	Ph36 Pt1
SiO_2	0.34	0.31	0.17	0.20	0.10	0.00	36.82	37.37	34.58	37.42	36.67	36.84	17.49
Al_2O_3	1.44	1.55	1.78	0.73	2.13	1.93	12.83	13.32	12.42	13.14	13.47	13.41	7.31
K_2O	–	–	–	–	–	–	8.54	8.94	8.58	9.19	8.79	8.66	3.42
Na_2O	–	–	–	–	–	–	0.57	0.54	0.52	0.54	0.48	0.43	0.00
CaO	–	–	–	–	–	–	0.14	0.25	0.05	0.07	0.18	0.31	0.18
FeO	77.97	78.65	82.82	85.32	82.55	82.99	18.71	17.13	24.39	19.71	18.23	18.04	49.28
MgO	0.09	0.05	0.00	0.06	0.14	0.06	12.02	12.30	9.68	11.02	10.19	10.41	6.85
MnO	1.33	1.09	0.90	0.88	1.31	1.29	1.19	1.15	1.04	1.24	3.14	3.27	0.72
TiO_2	10.18	9.47	3.99	2.99	6.64	5.84	4.33	4.57	4.13	4.17	4.39	4.48	11.30
F	–	–	–	–	–	–	0.00	0.00	0.00	0.05	0.00	0.00	0.00
Cl	–	–	–	–	–	–	0.00	0.00	0.00	0.00	0.00	0.00	0.00
Total	91.36	91.13	89.65	90.19	92.87	92.12	95.14	95.57	95.38	96.54	95.55	95.86	96.54
Ti/Fe	0.118	0.108	0.043	0.032	0.072	0.063	0.209	0.240	0.152	0.190	0.217	0.223	0.206
Mg/Mg+Fe	0.002	0.001	0.000	0.001	0.003	0.001	0.536	0.564	0.417	0.502	0.502	0.509	0.200
Magnetite	0.702	0.721	0.889	0.923	0.816	0.840							
Ulvospinel	0.298	0.279	0.111	0.077	0.184	0.160							

	Matrix				Pumice						
Oxide	Ph13 Pt1	Ph19 Pt1	Ph20 Pt1	Ph44 Pt1	Ph8 Pt1	Ph8 Pt2	Ph11 Pt1	Ph11 Pt2	Ph20 Pt1	Ph20 Pt2	Ph42 Pt1
SiO_2	71.30	86.42	64.93	67.63	71.52	91.74	85.91	88.62	67.21	85.25	90.42
Al_2O_3	14.63	8.58	17.43	17.94	15.53	4.75	8.12	5.88	17.32	9.71	5.68
K_2O	5.81	0.66	5.71	7.99	5.25	2.14	0.73	0.55	6.55	2.46	1.98
Na_2O	3.97	4.02	5.61	4.62	4.86	1.34	3.49	2.51	4.53	3.05	1.81
CaO	0.60	0.79	0.63	0.38	0.65	0.20	0.80	0.73	0.60	0.73	0.26
MgO	0.52	0.05	0.18	0.22	0.10	0.12	0.09	0.36	0.13	0.09	0.41
FeO	0.80	0.37	0.48	0.20	0.31	0.32	1.64	0.57	1.09	0.25	0.20
TiO_2	0.11	0.05	0.07	0.14	0.02	0.00	0.06	0.00	0.00	0.10	0.12
MnO	0.00	0.00	0.03	0.06	0.00	0.05	0.21	0.01	0.03	0.00	0.02
BaO	0.00	0.14	0.14	0.00	0.05	0.08	0.00	0.02	0.04	0.08	0.00
Total	97.75	101.07	95.21	99.17	98.30	100.75	101.01	99.24	97.51	101.70	100.89
Qz	21.94	55.81	8.17	8.40	20.33	73.41	58.51	69.02	13.09	53.60	69.30
Or	36.36	3.99	35.56	47.81	31.81	13.41	4.56	3.49	40.89	14.94	12.33
Ab	37.72	36.95	52.99	41.83	44.65	12.69	33.10	24.17	42.90	28.02	17.02
An	2.98	3.25	3.27	1.92	3.31	0.50	3.83	3.32	3.13	3.43	1.34

Table 5. Microprobe analyses for sample Tpt CW4.

	Sanidine										
Oxide	Ph3 Pt1	Ph3 Pt2	Ph3 Pt3	Ph3 Pt4	Ph12 Pt1	Ph12 Pt2	Ph12 Pt3	Ph13 Pt1	Ph14 Pt2	Ph14 Pt3	Ph17 Pt1
SiO_2	67.03	67.11	66.57	67.60	65.14	64.92	68.04	67.29	66.95	67.52	67.45
Al_2O_3	19.31	20.18	18.99	19.50	19.36	18.75	15.43	19.34	19.36	19.32	19.31
K_2O	9.48	9.34	9.64	9.08	10.39	10.36	5.26	9.99	9.50	9.69	7.61
Na_2O	4.98	4.89	4.59	5.08	3.76	3.82	4.43	4.48	4.73	4.71	5.68
CaO	0.34	0.28	0.53	0.43	0.25	1.17	1.00	0.33	0.37	0.32	0.46
MgO	0.04	0.03	0.01	0.06	0.06	0.05	0.35	0.02	0.04	0.02	0.04
TiO_2	0.32	0.00	0.00	0.06	0.00	0.02	0.14	0.00	0.03	0.03	0.08
FeO	0.11	0.12	0.12	0.15	0.07	0.06	0.90	0.18	0.15	0.13	0.10
BaO	0.06	0.00	0.00	0.13	1.28	1.13	0.59	0.07	0.13	0.16	0.00
Total	101.67	101.95	100.44	102.07	100.33	100.27	96.14	101.72	101.23	101.90	100.74
Qz	–	–	–	–	–	–	–	–	–	–	–
Or	54.73	54.97	56.53	52.99	63.63	60.47	41.07	58.54	55.93	56.67	45.82
Ab	43.63	43.64	40.87	44.92	35.11	33.81	52.37	39.83	42.26	41.75	51.84
An	1.64	1.39	2.60	2.10	1.26	5.72	6.56	1.64	1.82	1.59	2.35

	Sanidine										
Oxide	Ph21 Pt1	Ph21 Pt2	Ph22 Pt1	Ph22 Pt2	Ph22 Pt3	Ph22 Pt4	Ph23 Pt1	Ph33 Pt1	Ph33 Pt2	Ph33 Pt3	Ph33 Pt4
SiO_2	68.26	67.08	67.20	66.99	66.84	67.93	67.64	66.65	65.66	66.70	65.25
Al_2O_3	18.33	18.59	18.09	19.24	19.38	19.37	14.92	18.96	19.17	19.02	19.61
K_2O	10.52	10.31	9.50	9.88	8.98	9.12	7.98	9.38	9.50	9.39	9.22
Na_2O	4.16	4.36	4.55	4.57	5.08	4.87	3.35	4.81	4.72	4.93	4.79
CaO	0.19	0.18	0.52	0.40	0.42	0.52	0.32	0.44	0.36	0.41	0.46
MgO	0.03	0.11	0.06	0.03	0.02	0.04	0.47	0.05	0.06	0.04	0.04
TiO_2	0.00	0.10	0.04	0.00	0.00	0.07	0.23	0.11	0.14	0.00	0.04
FeO	0.12	1.16	0.21	0.13	0.17	0.14	2.98	0.26	0.24	0.21	0.18
BaO	0.06	0.00	0.11	0.09	0.00	0.10	0.00	0.00	0.05	0.00	0.00
Total	101.67	101.69	100.29	101.32	100.88	102.17	97.89	100.56	99.79	100.70	99.60
Qz	–	–	–	–	–	–	–	–	–	–	–
Or	61.91	59.92	56.41	57.65	52.73	53.83	59.83	55.01	56.06	54.56	54.68
Ab	37.15	39.18	40.98	40.41	45.21	43.61	38.12	42.81	42.18	43.42	43.04
An	0.94	0.89	2.61	1.94	2.06	2.56	2.04	2.18	1.77	2.02	2.28

	Sanidine									
Oxide	Ph34 Pt1	Ph34 Pt2	Ph34 Pt3	Ph34 Pt4	Ph39 Pt1	Ph39 Pt2	Ph39 Pt3	Ph39 Pt4	Ph39 Pt5	Ph39 Pt6
SiO_2	66.24	65.23	65.60	65.89	66.00	65.08	65.83	66.46	65.60	65.99
Al_2O_3	19.32	19.28	19.10	19.41	18.92	19.56	19.33	19.10	19.54	19.06
K_2O	9.38	9.39	9.14	8.86	9.81	9.32	9.37	9.56	9.13	9.73
Na_2O	4.94	4.85	4.93	5.13	4.85	4.84	5.09	5.00	5.11	4.77
CaO	0.33	0.36	0.38	0.42	0.50	0.58	0.52	0.36	0.52	0.50
MgO	0.00	0.00	0.01	0.04	0.05	0.03	0.06	0.00	0.04	0.00
TiO_2	0.00	0.00	0.00	0.07	0.03	0.00	0.03	0.00	0.04	0.00
FeO	0.15	0.21	0.17	0.14	0.15	0.12	0.17	0.42	0.13	0.15
BaO	0.16	0.10	0.09	0.09	0.17	0.23	0.00	0.12	0.00	0.09
Total	100.52	99.42	99.43	100.05	100.48	99.77	100.40	101.06	100.10	100.37
Qz	–	–	–	–	–	–	–	–	–	–
Or	54.70	55.10	53.98	52.18	55.80	54.37	53.47	54.78	52.75	55.96
Ab	43.68	43.15	44.11	45.77	41.84	42.78	44.03	43.47	44.73	41.62
An	1.62	1.75	1.91	2.05	2.36	2.85	2.50	1.75	2.53	2.42

Table 5. (Continued)

	Plagioclase									
Oxide	Ph4 Pt1	Ph4 Pt2	Ph4 Pt3	Ph4 Pt4	Ph6 Pt1	Ph6 Pt2	Ph6 Pt3	Ph28 Pt1	Ph28 Pt2	Ph28 Pt3
SiO_2	64.78	65.51	65.43	64.46	65.21	64.32	65.28	58.00	65.20	65.20
Al_2O_3	23.29	22.56	23.14	22.91	23.07	21.66	23.03	27.40	22.88	22.68
K_2O	1.15	1.12	1.18	1.18	1.17	1.14	1.02	0.41	1.28	1.13
Na_2O	8.58	8.67	8.28	8.72	8.67	8.51	8.66	6.26	8.77	8.65
CaO	3.67	3.80	4.03	3.55	3.66	3.74	3.71	8.34	3.63	3.50
MgO	0.25	0.04	0.03	0.00	0.00	0.04	0.05	0.06	0.03	0.09
TiO_2	1.07	0.00	0.07	0.00	0.08	0.00	0.00	0.02	0.07	0.04
FeO	0.02	0.12	0.15	0.19	0.13	0.15	0.00	0.14	0.14	0.19
BaO	0.00	0.00	0.04	0.07	0.03	0.04	0.07	0.09	0.00	0.00
Total	102.81	101.81	102.36	101.08	102.02	99.60	101.82	100.74	101.99	101.49
Qz	–	–	–	–	–	–	–	–	–	–
Or	6.66	6.41	6.91	6.80	6.71	6.62	5.91	2.45	7.26	6.57
Ab	75.48	75.34	73.33	76.04	75.62	75.12	76.04	56.14	75.44	76.33
An	17.86	18.25	19.76	17.16	17.67	18.26	18.05	41.41	17.30	17.10

	Plagioclase											
Oxide	Ph29 Pt1	Ph29 Pt2	Ph29 Pt3	Ph29 Pt4	Ph32 Pt1	Ph32 Pt2	Ph32 Pt3	Ph32 Pt4	Ph35 Pt1	Ph35 Pt2	Ph35 Pt3	Ph35 Pt4
SiO_2	65.75	65.02	64.77	65.58	62.92	63.82	64.89	64.52	64.38	64.07	63.79	64.00
Al_2O_3	21.76	22.21	22.94	22.50	22.72	23.32	22.90	22.63	22.91	22.80	23.12	22.65
K_2O	1.62	1.43	1.15	1.25	1.17	1.11	1.22	0.90	1.09	1.09	1.01	1.01
Na_2O	8.81	8.61	8.42	8.88	8.47	8.49	8.76	8.59	9.25	8.98	9.10	9.13
CaO	2.83	3.30	3.85	3.11	3.64	3.73	3.46	3.89	3.40	3.40	3.66	3.64
MgO	0.03	0.02	0.04	0.04	0.03	0.04	0.04	0.04	0.00	0.00	0.00	0.00
TiO_2	0.00	0.00	0.00	0.02	0.02	0.05	0.00	0.05	1.07	0.05	0.06	0.04
FeO	0.21	0.20	0.12	0.25	0.23	0.23	0.19	0.24	0.17	0.17	0.78	0.17
BaO	0.07	0.00	0.00	0.03	0.00	0.00	1.88	0.00	0.11	0.02	0.00	0.00
Total	101.08	100.78	101.28	101.66	99.20	99.79	103.33	100.86	102.38	100.57	101.51	100.65
Qz	–	–	–	–	–	–	–	–	–	–	–	–
Or	9.36	8.27	6.72	7.19	6.85	6.47	6.99	5.25	6.06	6.20	5.65	5.63
Ab	76.97	75.67	74.45	77.73	75.27	75.23	76.32	75.76	76.06	77.56	77.18	77.29
An	13.68	16.05	18.82	15.08	17.88	18.30	16.69	19.00	15.89	16.24	17.17	17.07

	Plagioclase			
Oxide	Ph36 Pt1	Ph36 Pt2	Ph36 Pt3	Ph36 Pt4
SiO_2	55.90	56.09	56.49	55.96
Al_2O_3	28.45	27.88	27.72	28.57
K_2O	0.25	0.43	0.49	0.32
Na O	5.84	6.26	6.38	5.96
CaO	9.58	9.06	8.49	9.55
MgO	0.02	0.02	0.02	0.19
TiO_2	0.00	0.04	0.02	0.01
FeO	0.35	0.31	0.27	0.28
BaO	0.12	0.17	0.12	0.17
Total	100.50	100.27	99.99	101.02
Qz	–	–	–	–
Or	1.47	2.47	2.82	1.86
Ab	51.65	54.13	55.99	52.03
An	46.88	43.40	41.20	46.11

	Biotite						
	Ph1 Pt1	Ph1 Pt2	Ph1 Pt3	Ph1 Pt4	Ph2 Pt1	Ph2 Pt2	Ph2 Pt3
SiO_2	37.99	36.98	37.43	36.38	33.56	30.74	33.54
Al_2O_3	13.11	12.98	12.63	12.98	13.44	13.27	13.34
K_2O	9.11	8.76	8.88	8.71	7.38	7.08	6.76
Na_2O	0.63	0.95	0.50	0.48	0.54	0.34	0.93
CaO	0.15	0.16	0.23	0.19	0.28	0.25	0.29
FeO	18.50	20.19	18.20	17.89	19.18	22.65	22.19
MgO	11.77	12.25	11.40	11.44	12.84	12.09	9.56
MnO	0.72	0.71	0.75	0.76	1.24	1.43	1.13
F	0.00	0.05	0.04	0.00	0.07	0.05	0.04
Cl	0.00	0.00	0.00	0.00	0.00	0.00	0.00
Total	96.21	97.45	94.03	93.08	92.94	92.02	91.86
Ti/Fe	0.206	0.196	0.197	0.214	0.207	0.164	0.166
Mg/Mg+Fe	0.534	0.522	0.530	0.535	0.547	0.490	0.437

Table 5. (Continued)

	Biotite										Magnetite	
Oxide	Ph16 Pt1	Ph16 Pt?	Ph16 Pt3	Ph16 Pt4	Ph25 Pt1	Ph25 Pt2	Ph25 Pt3	Ph37 Pt1	Ph37 Pt2		Ph8 Pt1	Ph8 Pt2
SiO_2	32.96	36.73	36.44	31.44	37.32	31.64	36.74	32.43	34.42	SiO_2	0.32	0.86
Al_2O_3	11.92	12.95	12.83	11.55	13.30	11.49	13.31	11.35	11.98	Al_2O_3	0.71	0.58
K_2O	7.73	8.62	8.51	7.22	8.77	7.17	8.06	8.10	8.25	K_2O	–	–
Na_2O	0.46	0.51	0.52	0.32	0.53	0.42	0.51	0.39	0.57	Na_2O	–	–
CaO	0.53	0.31	0.44	0.79	0.15	0.14	0.32	0.26	0.36	CaO	–	–
FeO	22.94	18.30	18.83	25.32	18.29	29.96	23.21	24.89	20.23	FeO	84.29	83.62
MgO	10.59	12.15	11.77	10.92	11.49	9.96	11.67	8.93	9.54	MgO	0.14	0.21
MnO	1.27	1.44	1.26	1.27	1.44	1.31	1.39	0.83	0.89	MnO	1.90	2.21
TiO_2	4.43	4.40	4.61	3.46	4.38	4.49	4.11	3.64	4.94	TiO_2	2.02	1.99
F	0.04	0.00	0.04	0.00	0.54	0.00	0.09	0.00	0.00	F	–	–
Cl	0.00	0.00	0.00	0.00	0.00	0.00	0.90	0.00	0.00	Cl	–	–
Total	92.86	95.42	95.27	92.28	96.21	96.57	99.41	90.82	91.17	Total	89.37	89.39
Ti/Fe	0.174	0.217	0.220	0.123	0.216	0.135	0.159	0.132	0.220	Ti/Fe	0.022	0.022
Mg/Mg + Fe	0.454	0.544	0.529	0.437	0.531	0.374	0.475	0.393	0.459	Mg/Mg + Fe	0.003	0.005
										Magnetite	0.970	0.974
										Ulvospinel	0.030	0.026

	Magnetite						Ilmenite						
Oxide	Ph11 Pt1	Ph30 Pt1	Ph30 Pt2	Ph31 Pt1	Ph31 Pt2		Ph30 Pt1	Ph30 Pt2	Ph31 Pt1	Ph31 Pt2	Ph40 Pt1	Ph40 Pt2	Ph40 Pt3
SiO_2	0.57	0.29	0.34	0.24	0.30	SiO_2	0.39	0.16	0.24	0.27	0.52	0.53	1.01
Al_2O_3	0.95	0.72	0.68	0.62	0.72	Al_2O_3	0.04	0.03	0.03	0.03	0.02	0.00	0.06
K_2O	–	–	–	–	–	K_2O	–	–	–	–	–	–	–
Na_2O	–	–	–	–	–	Na_2O	–	–	–	–	–	–	–
CaO	–	–	–	–	–	CaO	–	–	–	–	–	–	–
FeO	81.29	81.49	78.90	79.60	80.55	FeO	45.76	45.35	46.14	44.06	44.81	45.11	46.43
MgO	0.11	0.10	0.10	0.16	0.17	MgO	0.19	0.10	0.22	0.16	0.44	0.36	0.35
MnO	0.59	1.59	1.81	1.49	1.25	MnO	3.71	4.20	4.22	4.72	6.20	5.80	5.24
TiO_2	5.49	8.93	9.09	9.43	9.79	TiO_2	48.06	49.12	48.69	48.92	47.22	47.31	42.24
F	–	–	–	–	–	F	–	–	–	–	–	–	–
Cl	–	–	–	–	–	Cl	–	–	–	–	–	–	–
Total	89.00	93.10	90.01	91.55	92.77	Total	98.15	98.07	99.53	98.17	99.22	99.11	94.33
Ti/Fe	*0.061*	*0.099*	*0.104*	*0.107*	*0.109*	*Ti/Fe*	*0.945*	*0.974*	*0.949*	*0.999*	*0.948*	*0.943*	*0.799*
Mg/Mg + Fe	0.002	0.002	0.002	0.004	0.004	Mg/Mg + Fe	0.008	0.004	0.009	0.007	0.017	0.014	0.013
Magnetite	0.837	0.755	0.746	0.734	0.723	Magnetite	0.923	0.935	0.919	0.939	0.885	0.890	0.807
Ulvospinel	0.163	0.245	0.254	0.266	0.277	Hematite	0.077	0.065	0.081	0.061	0.115	0.110	0.193

Table 5. (Continued)

	Pumice			Matrix		
	Ph7	PH41		Ph43	Ph44	Ph44
Oxide	Pt1	Pt1	Oxide	Pt2	Pt1	Pt2
SiO_2	94.04	95.68	SiO_2	64.73	83.86	87.68
Al_2O_3	0.44	1.53	Al_2O_3	20.98	9.83	7.24
K_2O	0.03	0.05	K_2O	8.72	5.28	2.70
Na_2O	0.24	0.66	Na_2O	4.29	2.33	2.29
CaO	0.13	0.26	CaO	0.43	0.23	0.44
MgO	0.02	0.03	MgO	0.14	0.05	0.05
MnO	0.00	0.00	MnO	0.05	0.06	0.02
TiO_2	0.00	0.02	TiO_2	0.08	0.00	0.00
FeO	0.04	0.00	FeO	0.31	0.22	0.11
BaO	0.00	0.00	FeO	0.00	0.00	0.00
Total	96.01	98.22	Total	99.72	101.85	100.52
Qz	97.28	92.40	Qz	4.80	46.40	60.64
Or	0.20	0.32	Or	52.67	31.68	16.56
Ab	2.48	6.50	Ab	39.31	21.22	21.26
An	0.30	0.78	An	2.18	0.71	1.54

Table 6. Microprobe analyses for sample Tpt CW7.

	Sanidine											
	Ph1	Ph1	Ph2	Ph2	Ph3	Ph3	Ph9	Ph9	Ph9	Ph10	Ph19	Ph19
Oxide	Pt1	Pt2	Pt1	Pt2	Pt1	Pt2	Pt1	Pt2	Pt3	Pt1	Pt1	Pt2
SiO_2	66.05	66.96	65.82	66.42	65.50	65.23	65.25	65.40	65.59	65.23	66.04	65.42
Al_2O_3	19.24	19.28	19.69	19.68	19.33	19.34	19.34	19.50	19.26	19.50	19.46	19.71
K_2O	10.41	10.76	10.12	9.37	10.36	10.55	10.53	10.41	10.15	10.19	9.16	9.72
Na_2O	4.93	4.46	4.45	5.12	4.33	4.48	4.28	4.36	4.44	4.51	4.96	4.72
CaO	0.21	0.16	0.38	0.56	0.26	0.28	0.23	0.22	0.24	0.26	0.43	0.37
MgO	0.00	0.05	0.00	0.00	0.00	0.00	0.00	0.00	0.00	0.00	0.00	0.00
TiO_2	0.00	0.04	0.00	0.05	0.00	0.00	0.03	0.00	0.05	0.00	0.00	0.03
FeO	0.10	0.12	0.15	0.11	0.06	0.09	0.09	0.07	0.08	0.12	0.13	0.13
BaO	0.02	0.00	0.00	0.11	0.19	0.07	0.11	0.00	0.05	0.22	0.00	0.00
Total	100.96	101.82	100.61	101.42	100.03	100.04	99.87	99.96	99.86	100.03	100.19	99.57
Qz	–	–	–	–	–	–	–	–	–	–	–	–
Or	57.64	60.92	58.90	53.20	60.43	60.05	61.17	60.49	59.41	59.10	53.77	56.53
Ab	41.40	38.30	39.23	44.12	38.31	38.64	37.70	38.42	39.39	39.65	44.09	41.64
An	0.96	0.78	1.86	2.68	1.27	1.31	1.12	1.09	1.19	1.25	2.14	1.83

	Sanidine							Plagioclase		
	Ph27	Ph27	Ph28	Ph28	Ph31	Ph31	Ph31	Ph2	Ph2	Ph2
Oxide	Pt1	Pt2	Pt1	Pt2	Pt1	Pt2	Pt3	Oxide	Pt1	Pt2	Pt3
SiO_2	66.94	65.55	65.60	66.31	66.71	66.69	65.94	SiO_2	64.43	60.79	61.04
Al_2O_3	18.96	18.88	19.60	18.82	19.25	19.23	19.13	Al_2O_3	23.12	24.97	25.32
K_2O	10.29	10.27	10.35	10.71	10.27	10.00	8.44	K_2O	1.53	0.74	0.66
Na_2O	4.28	4.45	4.43	4.23	4.44	4.46	5.47	Na_2O	8.73	7.85	7.80
CaO	0.16	0.15	0.19	0.18	0.15	0.18	0.60	CaO	2.95	5.47	5.70
MgO	0.00	0.00	0.00	0.00	0.00	0.00	0.00	MgO	0.00	0.00	0.03
TiO_2	0.02	0.00	0.03	0.03	0.04	0.00	0.00	TiO_2	0.01	0.00	0.00
FeO	0.06	0.06	0.08	0.04	0.03	0.07	0.03	FeO	0.19	0.21	0.17
BaO	0.05	0.02	0.00	0.00	0.00	0.00	0.00	BaO	0.00	0.08	0.00
Total	100.77	99.38	100.27	100.32	100.89	100.63	99.62	Total	100.96	100.10	100.72
Qz	–	–	–	–	–	–	–	Qz	–	–	–
Or	60.83	59.92	60.09	61.97	59.98	59.16	49.98	Or	8.89	4.32	3.83
Ab	38.39	39.34	38.97	37.15	39.28	39.96	48.10	Ab	76.76	69.05	68.49
An	0.78	0.75	0.94	0.88	0.73	0.88	2.93	An	14.35	26.64	27.68

Table 6. (Continued)

	Plagioclase											
Oxide	Ph7 Pt1	Ph7 Pt2	Ph7 Pt3	Ph14 Pt1	Ph14 Pt2	Ph14 Pt3	Ph15 Pt1	Ph15 Pt2	Ph15 Pt3	Ph32 Pt1	Ph32 Pt1	Ph32 Pt3
SiO_2	63.35	63.16	65.33	63.00	63.66	64.48	61.70	62.16	61.71	65.22	65.02	64.32
Al_2O_3	23.47	23.12	23.18	22.94	23.24	23.45	24.81	24.74	24.26	22.15	22.46	22.92
K_2O	1.08	1.10	1.10	1.29	1.14	1.31	0.80	0.90	0.90	1.48	1.35	1.36
Na_2O	8.74	8.66	9.54	8.60	8.66	8.59	7.90	8.19	8.28	8.89	8.97	8.87
CaO	3.83	3.81	3.44	3.69	3.75	3.49	5.48	4.96	4.86	2.99	2.97	3.22
MgO	0.02	0.00	0.02	0.02	0.02	0.01	0.02	0.02	0.03	0.00	0.02	0.03
TiO_2	0.00	0.04	0.03	0.00	0.00	0.01	0.00	0.00	0.00	0.03	0.00	0.03
FeO	0.18	0.17	0.20	0.14	0.55	0.20	0.12	0.11	0.11	0.19	0.15	0.13
BaO	0.00	0.00	0.00	0.00	0.00	0.00	0.00	0.00	0.00	0.00	0.00	0.00
Total	100.67	100.07	102.84	99.67	101.02	101.54	100.83	101.08	100.15	100.95	100.95	100.90
Qz	–	–	–	–	–	–	–	–	–	–	–	–
Or	6.15	6.33	5.94	7.38	6.54	7.61	4.61	5.13	5.13	8.48	7.74	7.76
Ab	75.53	75.33	78.40	74.86	75.38	75.1	68.94	71.03	71.59	77.14	77.98	76.80
An	18.32	18.34	15.66	17.76	18.08	16.99	26.46	23.85	23.28	14.39	14.28	15.44

	Plagioclase				Biotite								
Oxide	Ph33 Pt1	Ph37 Pt2	Ph37 Pt3		Ph6 Pt1	Ph6 Pt2	Ph7 Pt1	Ph7 Pt2	Ph8 Pt1	Ph8 Pt2	Ph12 Pt1	Ph12 Pt2
SiO_2	63.20	59.75	61.34	SiO_2	35.74	36.58	36.44	36.60	34.23	34.99	35.60	34.95
Al_2O_3	22.19	25.11	24.55	Al_2O_3	14.12	14.13	14.33	14.01	13.52	14.10	13.15	12.91
K_2O	1.52	0.63	0.74	K_2O	9.16	9.14	9.38	9.53	8.88	8.59	9.19	9.14
Na_2O	8.83	7.74	7.74	Na_2O	0.54	0.47	0.47	0.44	0.47	0.45	0.62	0.53
CaO	3.11	6.04	5.60	CaO	0.00	0.00	0.00	0.00	0.02	0.06	0.08	0.06
MgO	0.00	0.00	0.00	FeO	20.41	17.46	15.36	16.20	20.60	21.49	21.57	20.82
TiO_2	0.01	0.04	0.00	MgO	11.87	11.82	12.59	12.02	11.18	11.32	10.14	9.95
FeO	0.06	0.13	0.23	MnO	1.51	1.51	1.63	1.40	1.39	1.11	1.45	1.43
BaO	0.00	0.00	0.00	TiO_2	4.42	4.64	4.90	5.23	5.60	4.21	4.51	4.59
				F	0.00	0.08	0.12	0.07	0.09	0.11	0.09	0.00
Total	98.92	99.44	100.20	Cl	0.00	0.00	0.00	0.00	0.00	0.00	0.00	0.00
Qz	–	–	–	Total	97.78	95.82	95.23	95.50	95.95	96.42	96.40	94.38
Or	8.67	3.60	4.32									
Ab	76.44	67.32	68.33	Ti/Fe	0.195	0.239	0.287	0.291	0.245	0.176	0.188	0.198
An	14.89	29.09	27.35	Mg/Mg + Fe	0.511	0.549	0.596	0.572	0.494	0.487	0.458	0.462

Table 6. (Continued)

	Biotite				Ilmenite						Magnetite		
	Ph21	Ph21	Ph25		Ph16	Ph18	Ph18	Ph29	Ph29		Ph29	Ph29
Oxide	Pt1	Pt2	Pt1	Oxide	Pt1	Pt1	Pt2	Pt1	Pt2	Oxide	Pt1	Pt2
SiO_2	37.24	35.97	40.03	SiO_2	0.38	0.03	0.02	0.21	0.27	SiO_2	0.29	0.15
Al_2O_3	13.51	13.21	14.97	Al_2O_3	0.77	0.03	0.00	0.05	0.05	Al_2O_3	2.25	2.02
K_2O	9.34	9.14	9.58	K_2O	–	–	–	–	–	K_2O	–	–
Na_2O	0.51	0.50	0.68	Na_2O	–	–	–	–	–	Na_2O	–	–
CaO	0.17	0.22	0.00	CaO	–	–	–	–	–	CaO	–	–
FeO	14.12	15.50	11.22	FeO	42.95	46.94	47.43	44.42	40.23	FeO	83.13	82.22
MgO	12.73	12.81	12.68	MgO	0.18	0.30	0.28	0.15	0.22	MgO	0.07	0.03
MnO	2.36	2.45	1.39	MnO	7.71	3.82	3.53	5.51	7.54	MnO	1.62	1.70
TiO_2	5.15	4.61	5.05	TiO_2	44.64	48.53	48.93	48.18	48.36	TiO_2	4.41	3.80
F	0.10	0.08	0.09	F	–	–	–	–	–	F	–	–
Cl	0.00	0.00	0.00	Cl	–	–	–	–	–	Cl	–	–
Total	95.21	94.48	95.69	Total	96.63	99.66	100.20	98.52	96.67	Total	91.76	89.92
Ti/Fe	0.328	0.268	0.405	Ti/Fe	0.935	0.930	0.928	0.976	1.081	Ti/Fe	0.048	0.042
Mg/Mg + Fe	0.619	0.598	0.671	Mg/Mg+Fe	0.008	0.011	0.010	0.006	1.010	Mg/Mg + Fe	0.002	0.001
				Ilmenite	0.858	0.912	0.915	0.916	0.938	Magnetite	0.889	0.908
				Hematite	0.142	0.088	0.085	0.084	0.062	Ulvospinel	0.112	0.092

	Pumice			Matrix	
	Ph30	Ph30		Ph35	Ph35
Oxide	Pt1	Pt2	Oxide	Pt1	Pt2
SiO_2	80.79	85.30	SiO_2	76.79	77.05
Al_2O_3	11.31	8.77	Al_2O_3	12.54	13.13
K_2O	4.32	1.85	K_2O	6.59	6.19
Na_2O	3.27	3.28	Na_2O	2.87	3.62
CaO	0.35	0.54	CaO	0.23	0.33
MgO	0.00	0.01	MgO	0.02	0.00
FeO	0.42	0.41	FeO	0.14	0 17
TiO_2	0.00	0.00	TiO_2	0.04	0.02
MnO	0.00	0.07	MnO	0.00	0.01
BaO	0.00	0.00	BaO	0.00	0.07
Total	100.45	100.24	Total	99.21	100.60
Qz	42.30	55.84	Qz	32.57	29.37
Or	36.30	11.27	Or	39.92	36.86
Ab	30.01	30.66	Ab	26.32	32.68
An	1.26	2.12	An	1.18	1.10

Table 7. Microprobe analyses for sample Tpt CW8.

	Sanidine										
Oxide	Ph1 Pt1	Ph1 Pt2	Ph1 Pt3	Ph3 Pt1	Ph3 Pt2	Ph3 Pt3	Ph3 Pt4	Ph4 Pt1	Ph4 Pt2	Ph4 Pt3	Ph4 Pt4
SiO_2	67.23	66.13	66.86	66.88	66.24	66.97	66.65	66.36	66.87	66.72	66.52
Al_2O_3	19.35	18.83	18.87	18.68	18.77	19.45	19.02	19.09	19.57	19.01	19.13
K_2O	10.27	10.36	9.98	10.43	10.57	10.30	10.20	9.64	9.88	10.06	10.10
Na_2O	4.71	4.38	4.71	4.46	4.35	4.43	4.57	4.91	4.77	4.65	4.51
CaO	0.28	0.23	0.27	0.26	0.24	0.27	0.31	0.27	0.29	0.28	0.26
MgO	0.09	0.00	0.00	0.00	0.00	0.00	0.00	0.00	0.00	0.00	0.00
TiO_2	0.00	0.03	0.00	0.00	0.00	0.00	0.02	0.50	0.00	0.02	0.04
FeO	0.11	0.13	0.11	0.08	0.11	0.08	0.08	0.08	0.08	0.11	0.11
BaO	0.25	0.28	0.23	0.00	0.35	0.32	0.25	0.19	0.32	0.32	0.20
Total	102.28	100.38	101.03	100.79	100.64	101.83	101.06	101.04	101.78	101.18	100.88
Qz	–	–	–	–	–	–	–	–	–	–	–
Or	58.20	60.25	57.53	59.88	60.83	59.75	58.68	55.65	56.95	58.00	58.86
Ab	40.46	38.63	41.18	38.86	37.99	38.55	39.84	43.03	41.65	40.65	39.88
An	1.32	1.13	1.30	1.25	1.18	1.30	1.49	1.32	1.40	1.36	1.26

	Sanidine								
Oxide	Ph5 Pt1	Ph5 Pt2	Ph5 Pt3	Ph11 Pt1	Ph11 Pt2	Ph16 Pt1	Ph16 Pt2	Ph16 Pt3	Ph16 Pt4
SiO_2	65.44	66.55	66.91	66.97	66.63	66.16	67.20	64.89	67.43
Al_2O_3	19.01	19.19	19.41	18.91	19.95	18.17	17.93	18.80	18.86
K_2O	9.80	9.61	9.73	9.17	9.19	10.09	10.49	10.51	9.26
Na_2O	4.79	4.92	4.95	5.23	5.16	4.31	4.31	4.24	5.05
CaO	0.25	0.29	0.28	0.33	0.37	0.18	0.11	0.15	0.36
MgO	0.00	0.00	0.00	0.00	0.00	0.00	0.00	0.00	0.00
TiO_2	0.00	0.03	0.01	0.02	0.00	0.00	0.04	0.01	0.00
FeO	0.18	0.14	0.13	0.11	0.13	0.14	0.18	0.16	0.13
BaO	0.10	0.10	0.00	0.11	0.13	0.02	0.08	0.11	0.10
Total	99.56	100.82	101.42	100.86	101.55	99.03	100.35	98.89	101.19
Qz	–	–	–	–	–	–	–	–	–
Or	56.77	55.49	55.71	52.80	53.04	60.39	61.25	61.56	53.80
Ab	42.03	43.12	42.92	45.60	45.15	38.68	38.20	37.69	44.46
An	1.20	1.40	1.37	1.60	1.81	0.92	0.55	0.76	1.71

	Sanidine								Pumice	
Oxide	*Ph17* Pt1	*Ph17* Pt2	*Ph17* Pt3	*Ph17* Pt4	*Ph18* Pt1	*Ph18* Pt2	*Ph18* Pt3	*Ph18* Pt4	*Ph6* Pt1	*Ph13* Pt1
SiO_2	66.85	66.37	66.25	65.81	65.64	66.58	66.14	66.59	93.55	73.39
Al_2O_3	19.10	19.39	19.05	19.28	19.39	18.74	19.39	19.34	4.30	16.08
K_2O	10.18	10.66	10.67	10.16	9.85	9.70	9.45	9.53	0.43	2.84
Na_2O	4.71	4.20	4.38	4.61	4.81	5.03	5.14	5.18	1.81	5.32
CaO	0.32	0.19	0.23	0.25	0.32	0.30	0.31	0.36	0.27	2.45
MgO	0.00	0.00	0.00	0.00	0.00	0.00	0.00	0.00	0.07	0.04
TiO_2	0.00	0.14	0.00	0.02	0.02	0.04	0.02	0.04	0.00	0.04
FeO	0.12	0.11	0.14	0.12	0.14	0.15	0.14	0.15	0.17	0.98
BaO	0.11	0.20	0.25	0.37	0.20	0.19	0.08	0.00	0.00	0.56
MnO									0.00	0.00
Total	101.39	101.27	100.98	100.62	100.37	100.73	100.67	101.19	100.60	101.70
Qz	–	–	–	–	–	–	–	–	78.73	23.89
Or	57.88	62.02	60.94	58.57	56.61	55.19	54.01	53.88	2.71	17.05
Ab	40.58	37.04	37.94	40.24	41.86	43.38	44.52	44.41	17.15	48.37
An	1.54	0.93	1.12	1.20	1.54	1.43	1.47	1.72	1.40	10.68

Table 7. (Continued)

	Plagioclase									
Oxide	Ph10 Pt1	Ph10 Pt2	Ph10 Pt3	Ph10 Pt4	Ph19 Pt1	Ph19 Pt2	Ph19 Pt3	Ph19 Pt4	Ph19 Pt5	Ph19 Pt6
SiO_2	64.78	63.40	64.45	63.97	65.50	64.02	64.02	64.04	64.30	65.04
Al_2O_3	22.04	22.79	22.85	23.14	21.64	22.26	22.69	22.16	23.06	22.41
K_2O	1.52	1.34	1.25	1.19	1.44	1.26	1.33	1.20	1.18	1.43
Na_2O	9.32	9.16	8.92	8.89	9.22	8.98	8.98	9.18	9.04	9.26
CaO	2.85	3.58	3.48	3.70	2.93	3.76	3.63	3.27	3.57	3.31
MgO	0.00	0.00	0.00	0.00	0.00	0.00	0.00	0.00	0.00	0.00
TiO_2	0.04	0.00	0.00	0.00	0.03	0.00	0.00	0.00	0.02	0.03
FeO	0.15	0.18	0.16	0.13	0.18	0.15	0.17	0.16	0.13	0.19
BaO	0.00	0.16	0.17	0.00	0.11	0.05	0.14	0.19	0.00	0.14
Total	100.71	100.61	101.28	101.02	101.05	100.48	100.96	100.20	101.31	101.82
Qz	–	–	–	–	–	–	–	–	–	–
Or	8.45	7.37	7.07	6.68	8.03	7.01	7.39	6.74	6.62	7.85
Ab	78.32	76.16	76.44	75.84	78.20	75.50	75.68	77.89	76.62	76.93
An	13.24	16.47	16.50	17.48	13.77	17.49	16.93	15.36	16.76	15.23

	Matrix			Biotite					Magnetite	
Oxide	Ph0 Pt1	Ph0 Pt2	Ph0 Pt3	Oxide	Ph12 Pt1	Ph12 Pt2	Ph22 Pt1	Ph22 Pt2	Ph22 Pt3	Oxide	Ph9 Pt1	Ph9 Pt2
SiO_2	77.92	91.60	70.96	SiO_2	38.37	39.28	38.10	34.64	38.54	SiO_2	0.17	0.56
Al_2O_3	12.74	6.12	16.68	Al_2O_3	15.13	15.37	14.31	12.18	13.53	Al_2O_3	1.6.	1.58
K_2O	6.28	0.58	9.38	K_2O	9.07	9.85	9.63	8.39	9.67	K_2O	–	–
Na_2O	3.72	2.91	4.18	Na_2O	0.53	0.51	0.61	0.44	0.59	Na_2O	–	–
CaO	0.30	0.67	0.21	CaO	0.15	0.15	0.00	0.00	0.00	CaO	–	–
MgO	0.02	0.00	0.00	MgO	17.23	16.63	14.67	13.74	14.44	MgO	0.11	0.11
FeO	0.33	0.14	0.55	FeO	10.62	3.72	12.97	20.57	13.01	FeO	82.55	82.22
TiO_2	0.04	0.06	0.05	TiO_2	4.52	3.96	4.00	3.88	3.78	TiO_2	3.62	4.22
MnO	0.03	0.01	0.07	MnO	2.70	2.40	1.24	1.70	1.72	MnO	1.92	1.88
BaO	0.00	0.00	0.00	F	0.08	0.00	0.06	0.05	0.09	F	–	–
				Cl	0.00	0.00	0.00	0.00	0.00	Cl	–	–
Total	101.40	101.90	102.07	MnO	98.40	91.88	95.61	95.60	95 36	MnO	89.98	90.60
Qz	29.13	68.41	9.25	Ti/Fe	0.383	0.957	0.278	0.169	0.261	MnO	0.040	0.046
Or	36.67	2.28	53.39	Mg/Mg+Fe	0.745	0.889	0.671	0.546	0.666	Mg/Mg+Fe	0.002	0.002
Ab	32.95	26.69	36.05							Ulvospinel	0.082	0.101
An	1.25	2.62	1.31							Magnetite	0.918	0.899

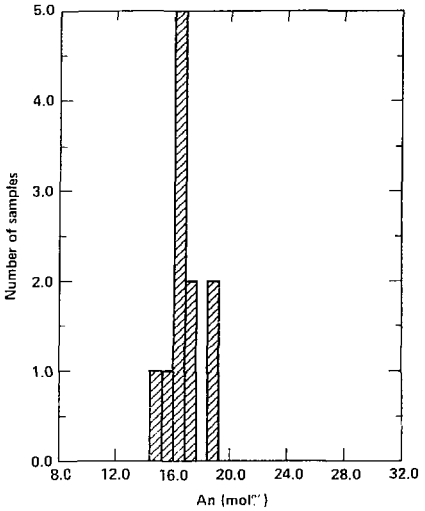

Figure 10. Ordinary histogram of calculated anorthite end-member composition determined by EMP analyses of the plagioclase feldspar phenocrysts on the reacted wafer Tpt CW3.

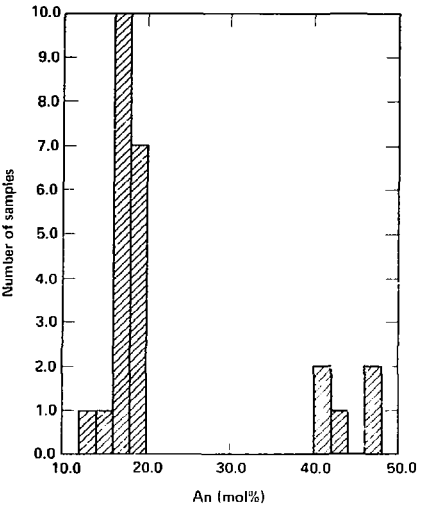

Figure 11. Ordinary histogram of calculated anorthite end-member composition determined by EMP analyses of the plagioclase feldspar phenocrysts on the reacted wafer Tpt CW4.

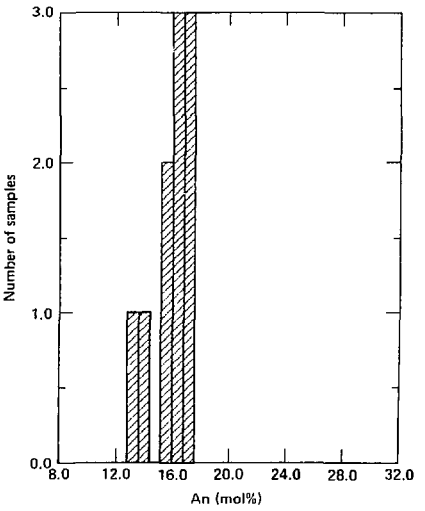

Figure 12. Ordinary histogram of calculated anorthite end-member composition determined by EMP analyses of the plagioclase feldspar phenocrysts on the reacted wafer Tpt CW8.

was true for both the fully submerged experiments and those run in water-saturated air. Table 8, which contains examples of typical analyses of each phase, shows that the overall chemical compositions were also similar.

3. The alkali feldspar phenocrysts were similarly unaffected by reaction and the calculated orthoclase end-member compositions are nearly identical (Table 8).

4. The biotites within the Topopah Spring tuff were badly altered (to oxides) even in the unreacted wafer, and analysis of the reacted biotites was difficult because of their rough surface texture. In those phenocrysts that yielded acceptable oxide totals in analysis, however, Table 9 shows no discernible difference before or after reaction. Biotite is the phase most obviously affected by reaction, and the lack of evidence in compositional change may be an artifact of the acceptable (high) oxide totals, simply meaning less severe alteration and hence a smoother surface with less chemical evidence of change (Knauss, 1984a).

5. The matrix compositions (see Table 9) were also unchanged, although it is not possible to quantitatively distinguish compositional variations in the devitrified matrix with EMP, since it can vary from silica to sanidine on a micron scale. Where the matrix was more coarsely devitrified, the individual phases were easily analyzed quantitatively. A comparison of a coarsely devitrified matrix before and after reaction also showed no evidence of compositional differences.

6. The only secondary phase observed was abundant calcite (see Fig. 13) that appeared in all the fully submerged experiments regardless of the extent of reaction with J-13 water. The calcite frequently attached to rough surfaces of phenocrysts (Fig. 14) or to vugs on the surface of the wafer (Fig. 15). The individual calcite masses most commonly consisted of groups of well-terminated, twinned crystals overgrown by a calcite cement that was not well-crystallized. In rare cases, single calcite crystals lacked the calcite cement coating (Fig. 16). Both the well-crystallized calcite and the calcite cement displayed evidence of dissolution. The SEM observations suggest that the calcite crystals grew relatively slowly (at least slowly enough for well-terminated, euhedral crystals to form), and that a rapid deposition of the calcite cement followed this slow growth. Subsequently, both the cement and the calcite crystals were subject to dissolution. This sequence of events may correspond to slow growth during the course of the experiment, deposition of the cement upon opening of the still somewhat warm bombs with the consequent rapid degassing of most of the remaining CO_2, and dissolution of both calcite phases upon cooling as a result of the retrograde solubilty of calcite.

7. The calcite produced in these experiments was fairly large, frequently up to several tens of microns in size, and we determined its composition in the following way: Individual calcite masses were hand-picked from the surface of

Table 8. Representative analyses of feldspar phenocrysts from the Tpt wafers.

	Plagioclase (wt%)			Alkali feldspar (wt%)		
Oxide	CW0	CW4	CW8	CW0	CW4	CW8
SiO_2	63.90	64.32	64.02	66.06	66.57	65.44
Al_2O_3	22.13	21.66	22.26	18.40	18.99	19.01
K_2O	1.24	1.14	1.26	10.14	9.64	9.80
Na_2O	8.65	8.51	8.98	4.38	4.59	4.79
CaO	3.53	3.74	3.76	0.11	0.53	0.25
MgO	0.00	0.04	0.00	0.00	0.01	0.00
FeO	0.00	0.15	0.15	0.18	0.12	0.18
TiO_2	0.00	0.00	0.00	0.06	0.00	0.00
BaO	0.02	0.04	0.05	0.15	0.00	0.10
Total	99.48	99.60	100.48	99.47	100.44	99.56
Orthoclase	7.17	6.62	7.01	60.07	56.53	56.77
Albite	75.73	75.12	75.50	39.37	40.87	42.30
Anorthite	17.10	18.26	17.49	0.56	2.60	1.20

Table 9. Representative analyses of biotite phenocrysts and matrix from the Tpt wafers.

	Biotite (%)			Matrix		
Oxide	CW0	CW4	CW8	CW0	CW4	CW8
SiO_2	36.45	36.98	34.64	73.64	83.86	77.92
Al_2O_3	13.15	12.98	12.18	13.73	9.83	12.74
K_2O	8.56	8.76	8.39	7.90	5.28	6.28
Na_2O	0.56	0.95	0.44	2.82	2.33	3.72
CaO	0.05	0.16	0.00	0.16	0.23	0.30
MgO	10.99	12.25	13.74	0.05	0.05	0.02
FeO	20.96	20.19	20.57	0.11	0.21	0.33
TiO_2	4.38	1.40	3.88	0.07	0.00	0.04
MnO	1.93	0.71	1.70	0.01	0.06	0.03
BaO	–	–	–	0.04	0.00	0.00
F	0.05	0.05	0.05	–	–	–
Cl	0.00	0.00	0.00	–	–	–
Total	97.08	97.44	95.60	99.53	101.85	101.38
Quartz	–	–	–	25.37	46.40	29.13
Orthoclase	–	–	–	48.08	31.68	36.67
Albite	–	–	–	26.04	21.22	32.95
Anorthite	–	–	–	0.51	0.71	1.25

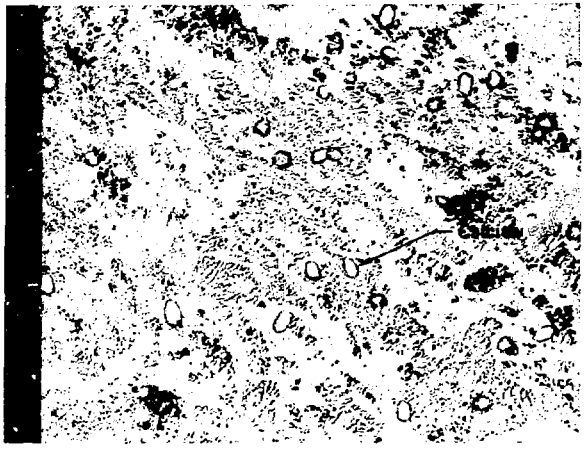

Figure 13. Scanning electron microscope back-scattered electron image of the surface of a reacted wafer showing the widespread distribution of secondary calcite.

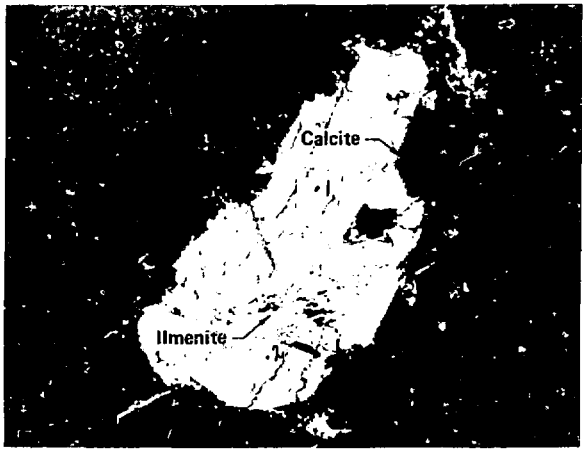

Figure 14. Scanning electron microscope back-scattered electron image of euhedral calcite plus cement growing on the surface of an ilmenite phenocryst.

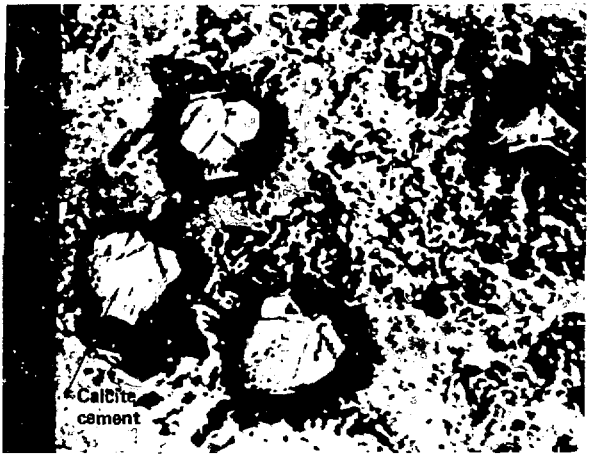

Figure 15. Scanning electron microscope back-scattered electron image of euhedral calcite plus cement growing on the rough surface of the wafer attached to the vugs present in the matrix.

Figure 16. Scanning electron microscope back-scattered electron image of euhedral calcite with cement and euhedral calcite without cement. Note the evidence of solution on both the euhedral calcite and the calcite cement, as well as the minor crystallographic ordering displayed by the cement that grew over the twinned calcite.

the reacted wafer and a polished grain mount was prepared. The calcite was then analyzed by quantitative WDS analysis. The calcite was large enough for at least two analyses to be made on each of a number of grains. Efforts were made to minimize beam damage to the calcite grains during analysis, although damage was seen in all cases. The normalized results are presented in Table 10. Although minor amounts of other oxides were sometimes present (silicon, aluminum, titanium), the grains were entirely magnesian calcite. There was a clear trend for the centers of the grains to contain higher magnesium oxide, which would agree with the aqueous phase results that show the solutions to become depleted in magnesium more rapidly than in calcium.

The effects of continuous degassing of volatiles through the Teflon on the solid phase SEM observations and EMP analyses presented above can be seen by comparison with the subsequent analogous Dickson-type gold-cell rocking autoclave experiments (as was done with the aqueous results previously presented). In the rocking autoclave experiments the solid phase observations made on wafers reacted for 64 days showed a number of significant differences from the observations made here. Although a few small, extensively corroded calcite grains were seen, they were largely replaced with silicon and they were much less numerous than the other secondary phases observed. The dominant secondary phases were illite and clay (rich in either magnesium, calcium, and/or iron). Other minor phases were kaolinite, gibbsite, and a pure-silicon phase (cristobalite?). In total, the amount of secondary material produced in the rocking autoclave experiments was much smaller than that produced in the Teflon-lined static autoclaves.

All of these differences between the solid phase observations in the rocking autoclaves and the Teflon-lined autoclaves are thought to be due to the continuous degassing of CO_2 through the Teflon. Consider the two equations below and the following working hypotheses:

$$HCO_3^- \rightarrow CO_2 \uparrow + OH^- \quad , \qquad (1)$$

$$Ca^{+2} + HCO_3^- \rightarrow CaCO_3 \downarrow + H^+ \quad . \qquad (2)$$

The continuous and relatively slow loss of volatiles through the Teflon results in the production of hydroxyl ion (1). The carbonate system buffers this effect by precipitating calcite (2). If these were the only reactions, the result would be the slow growth of calcite, the lowering of the alkalinity, and no change in pH. However, we observe a significant increase in the pH, which may be because reaction (2) is kinetically inhibited and hence lags behind reaction (1). It may also be because other H^+ consuming reactions are taking place, such as the hydrolysis of feldspars:

$$KAlSi_3O_8 + H^+ \rightarrow HAlSi_3O_8 + K^+ \quad . \qquad (3)$$

Reactions (1) through (3) could explain the formation of euhedral calcite, the lowering of alkalinity, and the observed increase in pH.

The formation of the calcite cement and subsequent dissolution of euhedral calcite and cement may be due to the following sequence of events. After the bombs were removed from the oven they were allowed to cool until they were

Table 10. Microprobe analyses of a calcite grain mount using secondary calcite picked from the surface of a reacted wafer

Oxide	Ph2 Pt1 Center	Ph2 Pt2 Edge	Ph3 Pt1 Center	Ph3 Pt2 Center	Ph3 Pt3 Edge	Ph4 Pt1 Center	Ph4 Pt2 Edge	Ph12 Pt1 Center	Ph12 Pt1 Edge	Ph15 Pt1 Center	Ph15 Pt2 Edge
SiO_2	0.42	0.05	0.15	0.00	0.04	0.16	0.03	0.18	0.10	0.00	0.04
Al_2O_3	0.34	0.00	0.16	0.03	0.09	0.79	0.06	0.29	0.03	0.05	0.03
FeO	0.03	0.03	0.29	0.02	0.00	0.00	0.06	0.00	0.00	0.05	0.00
MgO	2.78	1.16	1.65	1.41	1.23	1.52	0.62	2.24	0.89	1.53	0.64
MnO	0.07	0.00	0.06	0.00	0.00	0.11	0.00	0.03	0.04	0.07	0.00
CaO	96.37	98.24	97.60	98.09	97.55	97.35	98.79	95.89	98.81	98.31	99.02
BaO	0.00	0.18	0.10	0.12	0.00	0.07	0.11	0.29	0.00	0.00	0.04
Na_2O	0.00	0.00	0.00	0.11	0.00	0.00	0.00	0.00	0.00	0.00	0.00
K_2O	0.00	0.00	0.00	0.00	0.00	0.00	0.00	0.00	0.04	0.00	0.00
Ti_2O	0.00	0.06	0.00	0.04	0.83	0.00	0.00	1.08	0.10	0.00	0.04
SrO_2	–	0.10	–	0.19	0.27	–	0.32	–	0.00	–	0.20

still somewhat warm but cool enough to be disassembled and then opened. Possibly, upon opening the bombs, the still slightly warm solution could rapidly degas some of the remaining CO_2 and as Eqs. (1) and (2) above demonstrate, which could then result in the rapid deposition of a calcite cement. As the solution cooled the euhedral calcite and the calcite cement might have redissolved as a result of the retrograde solubility of calcite.

Summary

This report has presented the results of a series of preliminary experiments to determine the effects of the hydrothermal interaction of J-13 water with Topopah Spring tuff. The experiments were run in Teflon-lined, static autoclaves at 150°C for 120 days using polished wafers. The use of these wafers allowed the quantitative analyses of solid phases before and after reaction and the identification of any secondary minerals produced (by direct observation rather than by inference from water chemistry changes) as well as the quantitative analyses of quenched aqueous samples following reaction for specific time intervals. Samples were run either fully submerged in J-13 water or in water-saturated air with enough excess water present to allow refluxing. Outcrop samples were used to provide baseline values for Waste Package experimenters who must use outcrop material and to provide an approximation for results obtainable using actual drillcore material taken from appropriate depths beneath Yucca Mountain.

The results are preliminary in the sense that the experiments were conducted before the installation of a hydrothermal experimental facility using gold-cell rocking autoclaves and before an extensive set of experiments was subsequently run using drillcore material. Differences between the results obtained using the Teflon-lined autoclaves and those later obtained using the Dickson-type gold-cell rocking autoclaves have been noted.

The aqueous results show that for the fully submerged experiments, the changes in J-13 water composition produced by reaction are slight. The major change is an increase in dissolved silicon and minor increases in aluminum, potassium, sodium, and the anions. The increase in sodium and all the anions is partly due to the dissolution of a readily soluble component of evaporite minerals. The concentrations of calcium and magnesium decrease. There is also an increase in pH in these experiments, but that has been suggested to be the result of degassing and loss of volatiles (e.g., CO_2) through the Teflon rather than the result of reaction with the rock.

The aqueous results for the water-saturated air experiments show that the changes in J-13 water composition produced by reaction are even less significant than in the fully submerged experiments. Only the 120-day experiment produced any change in the silicon content, suggesting little interaction between the rock and water. The aluminum and iron were essentially removed from solution and the calcium decreased to even lower values than those seen in the fully saturated experiments. The potassium rose slightly, while the sodium and anion contents were very similar to those seen in the fully saturated experiments. This suggests that the readily soluble evaporite component present in these outcrop samples is removed even by the refluxing action in the water-saturated air experiments. The pH also rose as a result of the CO_2 degassing through the Teflon.

The solid phase analyses of primary phases (phenocrysts and matrix) show that the gross compositions (as determined by EMP) were unchanged by reaction with J-13 water at 150°C for 120 days. The only secondary phase observed was abundant euhedral magnesian calcite that was later coated by a calcite cement. Its production in abundance in these experiments in Teflon-lined autoclaves (at the expense of the suite of secondary minerals seen in analogous experiments run later in the Dickson-type gold-cell rocking autoclaves) is thought to be another result of the degassing of CO_2 through the Teflon.

The net result of these experiments is the expectation that the hydrothermal interaction of Topopah Spring tuff with water present in near-field surrounding a repository will produce a water whose composition differs only slightly from the starting composition. Furthermore, the rock itself is little affected by the interaction at these low temperatures. Although these experiments were preliminary and the specific details concerning water composition and secondary mineral production have been largely superseded by subsequent experiments using Dickson-type gold-cell rocking autoclaves, the general conclusions have been substantiated.

Acknowledgments

Many people helped with the experimental work presented in this report. Chuck Slettevold and Suzie Saunders made the BET gas adsorption measurements. Jan Brown helped with the sampling. Art Langhorst made the ICP-ES cation analyses. Jackie Lam made the IC anion analyses. Rick Ryerson kept the ES Department microprobe facility in top operating condition. Virginia Oversby offered many valuable constructive criticisms. Tom Wolery provided geochemical insight.

References

Knauss, K. G., V. M. Oversby, and T. J. Wolery (1983), "Post Emplacement Environment of Waste Packages," *Mat. Res. Soc. Symp. Proc.* **26**, pp. 301–308.

Knauss, K. G. (1984a), *Hydrothermal Interaction Studies of Bullfrog Member Tuff Core Wafers in J-13 Water at 150°C—Quantitative Analyses of Aqueous and Solid Phases*, Lawrence Livermore National Laboratory, Livermore, Calif., UCRL-53521.

Knauss, K. G. (1984b), *Petrologic and Geochemical Characterization of the Topopah Spring Member of the Paintbrush Tuff: Outcrop Samples Used in Waste Package Experiments*, Lawrence Livermore National Laboratory, Livermore, Calif., UCRL-53558.

Knauss, K. G., J. D. Delany, W. J. Beiriger, and D. W. Peifer (1984) *Hydrothermal Interaction of Topopah Spring Tuff with J-13 Water as a Function of Temperature*, accepted for publication in *Mat. Res. Soc. Symp. Proc.*, UCRL-90853.

Oversby, V. M. and K. G. Knauss (1983), *Reaction of Bullfrog Tuff with J-13 Water at 90°C and 150°C*, Lawrence Livermore National Laboratory, Livermore, Calif., UCRL-53442.

Oversby, V. M. (1984), Reaction of Topopah Spring Tuff with J-13 Well Water at 90°C and 150°C, Lawrence Livermore National Laboratory, Livermore, Calif., UCRL-53552.

Wolery, T. J. (1984), Lawrence Livermore National Laboratory, Livermore, Calif., private communication.